GEOLOGICA CARPATHICA, AUGUST 2016, 67, 4, 371–389 doi: 10.1515/geoca-2016-0023

Pleistocene volcaniclastic units from North-Eastern Sicily (Italy): new evidence for calc-alkaline explosive volcanism in the Southern Tyrrhenian Sea

MARCELLA DI BELLA[1], FRANCESCO ITALIANO[2], GIUSEPPE SABATINO[1], ALESSANDRO TRIPODO[1], ANGELA BALDANZA[3], SERGIO CASELLA[1], PAOLO PINO[1], RICCARDO RASA'[1] and SELMA RUSSO[1]

[1]Dipartimento di Scienze Matematiche e Informatiche, Scienze Fisiche e Scienze della Terra, Università di Messina, Viale F. Stagno d'Alcontres 31, 98166 Messina, Italy; mdibella@unime.it
[2]Istituto Nazionale di Geofisica e Vulcanologia, Palermo, Italy
[3]Dipartimento di Fisica e Geologia, Università di Perugia, Via A. Pascoli, 06123 Perugia, Italy

(Manuscript received June 30, 2015; accepted in revised form June 7, 2016)

Abstract: A well-preserved volcaniclastic sequence crops out in Pleistocene marine sediments along the Tyrrhenian coastline of the Calabrian-Peloritani arc (Sicily, Italy), testifying the occurrence of Lower-Middle Pleistocene volcanic activity in Southern Tyrrhenian Sea. The presence of dominant highly vesicular and minor blocky glassy particles indicates that the volcanic clasts were originated by explosive events related to the ascent and violent emission of volatile-rich magmas accompanied by and/or alternated with hydromagmatic fragmentation due to magma-sea water interaction. Field investigations and sedimentological features of the studied volcaniclastic units suggest a deposition from sediment-water density flows. The chemical classification of the pumice clasts indicates prevalent rhyolitic and dacitic compositions with calc-alkaline to high-K calc-alkaline affinity. The geochemical features of immobile trace elements together with the presence of orthopyroxene are indicative of a provenance from an arc-type environment. The age (from 980-910 to 589 ka), the chemical composition and the evidence of subaerial explosive volcanic activity constrain the origin nature and temporal evolution of the arc-type volcanism in the Southern Tyrrhenian domain. Finally, the new information here provided contribute to a better understanding of the temporal geodynamic evolution of this sector of the Mediterranean domain.

Key words: volcaniclastic deposits, Pleistocene volcanism, N-E Sicily, stratigraphy, explosive volcanic activity, Arc volcanism.

Introduction

The southern Tyrrhenian Sea is dotted with active volcanoes and seamounts generated by the subduction of the Ionian oceanic crust beneath the Calabrian-Peloritani Arc (e.g., Barberi et al. 1974; Beccaluva et al. 1982, 1985). All of the structures were deeply studied during the past decades from the geophysical (Barberi et al. 1973; Ventura et al. 1999; Marani & Gamberi 2004), petrological (Selli et al. 1977; Savelli 1984; Trua et al. 2002), and geochemical (Caracausi et al. 2005; Heinicke et al. 2009, Lupton et al. 2011; Italiano et al. 2014) points of view. Despite the studies carried out so far, the geodynamic setting and the evolution of the Mediterranean basin is still a debated matter (e.g. Carminati et al. 2012, and references therein).

The SE Tyrrhenian Sea is bordered to the East by the Calabrian-Peloritani Arc, which is laterally segmented by major WNW-trending shear zones that have accommodated the rotational movements (Malinverno & Ryan 1986; Knott & Turco 1991) from the late Miocene (Van Dijk & Scheepers 1995) up to recent (Tansi et al. 2007). The Calabrian-Peloritani Arc has been affected by a rapid regional uplift since the Quaternary (Westaway 1993; Cucci 2004; Ferranti et al. 2006), accommodated by a tectonic extensional regime (Monaco & Tortorici 2000; Catalano et al. 2003) also confirmed by GPS measurements (Serpelloni et al. 2013). The volcanic activity is located along the main regional faults and apart from the volcanism of the Aeolian Islands no other recent active volcanic centres were known. Loreto et al. (2015) confirmed the existence of a buried volcano offshore Capo Vaticano (Calabrian Arc). That seamount, which is still venting volcanic volatiles, coincides with the volcanic edifice responsible for the nearby Pleistocene volcaniclastic units occurring inside the half-graben depressions of the Mesima-Gioia Tauro and Reggio Calabria basins (De Rosa et al. 2001, 2008).

A further well-exposed and well-preserved volcaniclastic sequence included in marine sediments, crops out along the Tyrrhenian coastline of the Calabrian-Peloritani Arc (Peloritani Mountains), referred to the Lower-Middle Pleistocene (Kézirian 1992a,b; Toussaint et al. 1999) and represents the most complete outcrop of the area although other minor scattered occurrences are reported nearby (Kézirian 1992a,b). Within the Strait of Messina area, similar sequences are also exposed along the Calabrian coast (Kézirian 1992a,b; Calanchi 1988; Leyrit et al. 1998, 1999; Toussaint et al.

1999) and in several sites of the Ionian and peri-Tyrrhenian Calabria (Cello et al. 1983; Toussaint et al. 1999; De Rosa et al. 2001, 2002; Bigazzi & Carobene 2004; Carobene et al. 2006; De Rosa et al. 2008). Since the Late Tortonian, extensive explosive volcanic activity took place in the Mediterranean area, with dispersion of pyroclastic products over a large portion of the basin and of continental Europe (Keller et al. 1978; Paterne et al. 1988; Pyle et al. 1998; Narcisi & Vezzoli 1999; Pouclet et al. 1999; Schmidt et al. 2002).

In the last years, some studies (De Rosa et al. 2008; Trua et al. 2010) have been focused on volcaniclastic layers interbedded in marine successions along the Italian peninsula. In contrast, no information exists on the volcaniclastic horizons cropping out over the north-eastern Sicilian coast, located in front of the Aeolian Islands.

This paper accounts for the results of a multidisciplinary study of the volcaniclastic deposits cropping out in the north-eastern Sicilian coast (Fig. 1) and includes field investigations, stratigraphic, sedimentology, SEM-EDS and geochemical analyses. The results help to constrain the type of eruption, the deposition and transport mechanisms, and the petrochemical features. The temporal range of the volcanic events has been constrained by age data (Lentini et al. 2000, 2008; Pino et al. 2007a,b; Carbone et al. 2008) from micro-fossil assemblages of the sedimentary clay succession in which the volcaniclastic units are interbedded. The results provide new information about the less studied Sicilian volcaniclastic deposits. Their identification and correlation are adopted as tools for the reconstruction of the sedimentary sequence and of the volcanic history in the area.

Geological setting

The investigated area is located along the Sicilian sector of the Calabrian-Peloritani arc close to the Tyrrhenian coastline, about 25 km south of the Aeolian Arc (Fig. 1). It is characterized by a prevalent homogeneous and continuous lithological sequence of poorly fossiliferous marly clays, with inter-layered volcaniclastic units.

This clayey sequence, reported as "Argille di Spadafora *Auctt*." (Lentini et al. 2008; Carbone et al. 2008), was originally assigned to the Pleistocene on the basis of foraminifera content (Lombardo 1980; Violanti 1989; Kézirian 1992a,b). The calcareous nannofossil associations with *Pseudoemiliania lacunosa, Gephyrocapsa oceanica* and *Gephyrocapsa* sp.3 (MNN19f biozone *sensu* Rio et al. 1990) allowed us to ascribe the clayey formation to the Middle Pleistocene (Di Stefano & Lentini, 1995; Lentini et al. 2000, 2008; Pino et

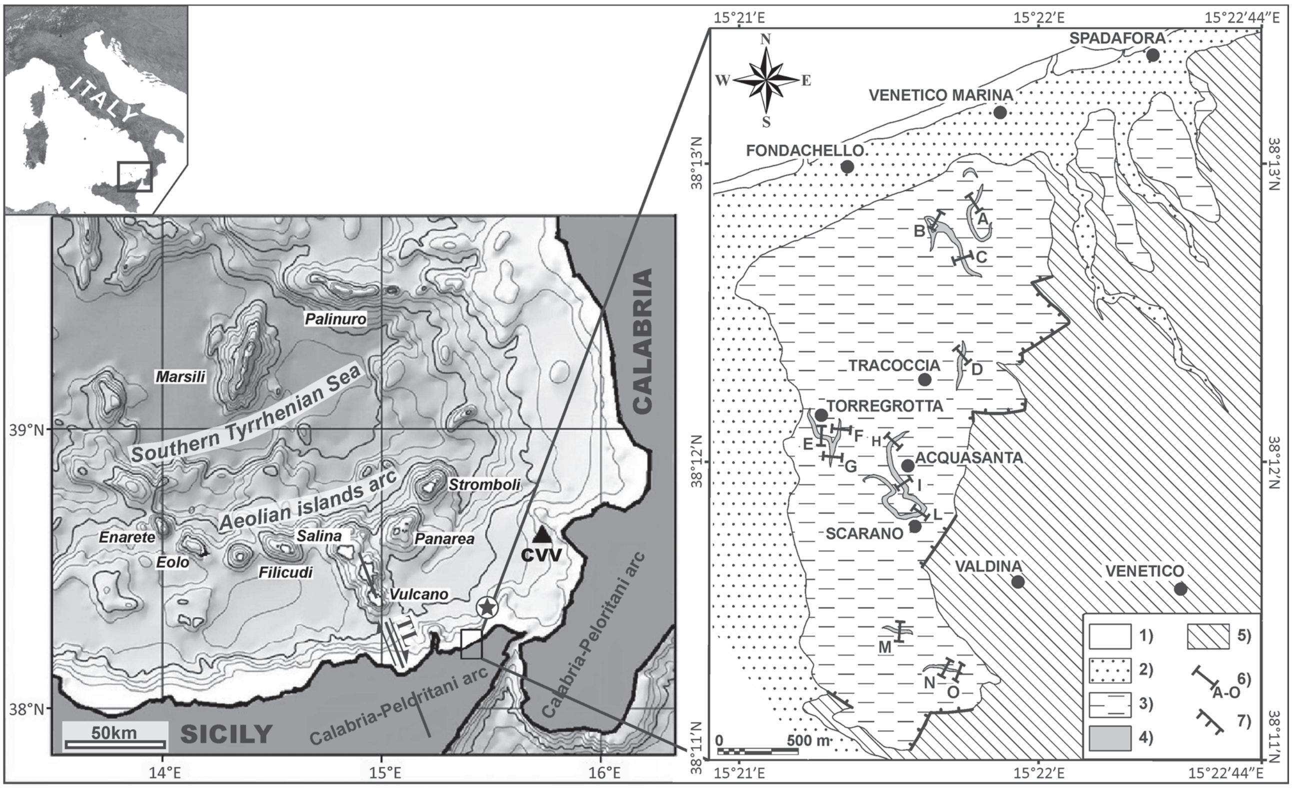

Fig. 1. Bathymetric map of the Southern Tyrrhenian Sea (following Kamenov et al. 2009, modified) on the left and geological sketch map of the study area showing the main outcropping formations and the volcaniclastic units (right). **Black star** — hypothetic volcanic edifice (Kezirian 1992a,b); **black triangle** — hypothesized volcanic edifice of Capo Vaticano (Loreto et al., 2015); **1** — beach deposits (Holocene); **2** — alluvial deposits (Holocene); **3** — gray-blue marly clay (Middle Pleistocene); **4** — volcaniclastic units; **5** — pre-Pleistocene substratum; **6** — traces of the stratigraphic sections; **7** — faults.

al. 2007a,b; Di Stefano in Carbone et al. 2008). The emplacement age of the marly-clayey sequence is constrained by the distribution of *Gephyrocapsa* sp.3 (*sensu* Rio et al. 1990; Pino et al. 2007a,b; Di Stefano in Carbone et al. 2008) that, in the Mediterranean Sea, covers a time interval from 980–910 to 589 ka (Castradori 1993; Sprovieri et al. 1998; Cita et al. 1998; Pino et al. 2007a,b). Based on published magnetostratigraphic data (criterion guide of Matuyama/Brunhes boundary: 0.78 Ma), the studied sequence has been attributed to the uppermost part of the Lower Pleistocene (Calabrian stage), corresponding to the top of the Jamarillo magnetic event, up to the lower part of the Middle Pleistocene (ex-Ionian stage *sensu* Cita et al. 2006). The estimated age fits that obtained by Cornette et al. (1987; from 1 to 0.72 Ma) for similar volcaniclastic units cropping out in the Reggio Calabria basin.

During this time interval, the deposition of deep-sea pelites in the deeper circalittoral to upper epi-bathyal zone (Kèzirian 1992a,b; Leyrit et al. 1998; Toussaint et al. 1999), up to 500–700 m below sea level, is testified by the foraminiferal benthonic assemblages recognized in similar clay marls cropping out in neighbouring localities (Violanti et al. 1987; Violanti 1988, 1989). These sedimentary deposits are preserved within a structural depression in areas adjacent to the present coastline. The substrate shows a siliciclastic (conglomeratic-arenaceous-clay) sequence (Gargano 1994; Lentini et al. 1995, 1997), Serravallian–Lower Messinian in age (Lentini et al. 2000), which was covered during Messinian times by discontinuous evaporitic carbonates (Gargano 1994; Lentini et al. 2000). Lower Pliocene marls and marly limestones (Trubi Formation) follow in the sequence. They are covered by limestone, sandy marls, organogenic sands and deep-water coral facies limestones attributed to the upper part of the Lower Pliocene up to Upper Pliocene (Gaetani & Saccà 1984; Barrier et al. 1987; Violanti et al. 1987; Violanti 1988; Di Stefano & Lentini 1995; Lentini et al. 2000; Pino et al. 2007a,b). The persistent tectonic activity caused, before clay sedimentation, a general uplift of the area up to the emersion and marine terrace formation (Lentini et al. 1996, Catalano & Cinque 1995).

During these latest phases, the marly clays pass into an alternating clay and sand sequence of circalittoral environment s.l. (Kézirian 1992a,b), and later to a 3rd and 4th order of fluvial and marine terraces (altitude of 90–220 m a.s.l.). They are related to the uppermost part of the Middle Pleistocene (isotopic stage 7) (Catalano & Cinque 1995, Catalano & Di Stefano 1997) and to the Tyrrhenian (isotopic stage 5) (Bonfiglio & Violanti 1984).

Multidisciplinary approach and analytical techniques

Field work

Eight volcaniclastic units (hereafter referred to as VU) were identified by field investigations. Thirteen stratigraphic sections have been reconstructed and correlated each other using the most widespread unit VU7 as a marker horizon (Fig. 2). Despite the fact that the volcaniclastic units are not exposed in all the sections, it was possible to establish correlations based on their lithological characteristics and stratigraphic position. A suite of fifty samples of volcanic sediments were collected and among all the pumice-rich units, the least altered samples were selected for laboratory work.

Detailed information on each volcaniclastic unit (VU) is reported in the result section.

Laboratory work

In the laboratory, the grain-size characteristics were determined by dry sieving at ½ϕ intervals, in the $-5<\phi<4$ size range. Sieving was carried out by hand to avoid excessive breakage of juvenile vesicular fragments. Statistical parameters, such as median diameter (Mdϕ), mean (Mϕ), graphical standard deviation (σϕ) and first-order skewness (αϕ), have been obtained by construction of cumulative curves as proposed by Inmann (1952).

In order to constrain the provenance and the processes involved in the fragmentation and alteration mechanisms, morphological investigations and mineral chemistry of the main representative phases and pumice particles (size ranging from 250 to 1100 µm) were performed by SEM-EDS (Sheridan & Wohletz 1983) focussed on the characterization of surface and vesicle structures. After selection, the pumice clasts were cleaned for a few seconds in ultrasonic bath and then mounted individually on a metal stub. Afterwards, a petrographic study was carried out to better define structure and composition of both pumice clasts and blackish lithics. Bulk rock analyses of twenty-one selected pumices were carried out by X-Ray Fluorescence to obtain geochemical information on the parental magma of the volcaniclastic sequence.

Analytical techniques

The chemical composition of minerals in selected pumice clasts was determined at the Physics and Earth Sciences SEM-EDS Laboratory of the Messina University. Analyses of Si, Al, Ti, Mn, Mg, Fe, Ca, Na, K, Cr and P contents were carried out using a LEO-S420 Electron Microscope coupled to an Oxford link ISIS series 3000 EDX spectrometer and Si(Li) detector with resolution of 156 eV at MnKα. Working distance 19 mm at acceleration voltage of 20 kV and 550 pA (PROBE). The spectral data were acquired at 1500 to 2000 counts/s with dead time below 25 %, using the ZAF correction.

The chemical analyses of pumice clasts were carried out at the Earth Sciences XRF laboratory at Perugia University. The samples were crushed in a steel jaw crusher and reduced to a fine powder in agate mortars. The concentrations of SiO_2, TiO_2, Al_2O_3, Fe_2O_3, MnO, CaO, K_2O, P_2O_5, Nb, Zr, Y, Sr, Rb, Ba, Cr, V, and Ni were measured by X-ray fluorescence on powder pellets using a wavelength-dispersive automated Philips PW1400 spectrometer. MgO and Na_2O

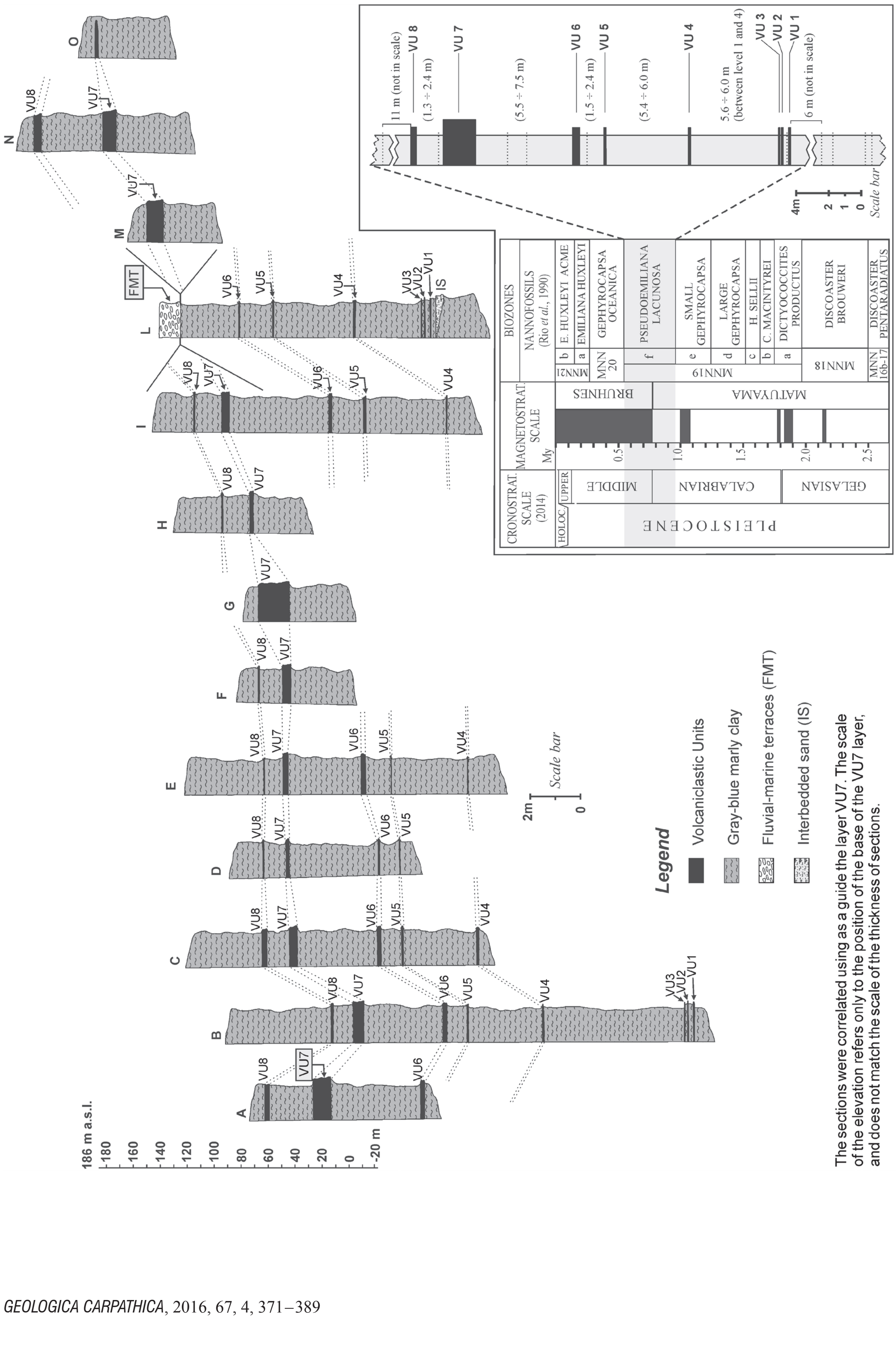

Fig. 2. Key stratigraphic sections of Middle Pleistocene clayey sequence with volcaniclastic deposits located in the geological map of Figure 1. **Inset:** generalized stratigraphic log showing the position of the studied volcaniclastic units.

concentrations were respectively determined by atomic absorption spectrophotometry and flame emission on sample solution after perchloric and hydrofluoric acid attack. FeO was determined by titration after rapid HF-H_2SO_4 attack. LOI (Loss on Ignition) is the weight loss after heating at 950 °C. Precision is better than 10 % for all trace elements.

Results

Detailed information on the volcaniclastic units

VU1, VU2 and VU3 crop out in the Scarano Locality (section L of Fig. 2) and nearby Venetico Village (section B of Fig. 2), where the lowest portion of the entire sequence is exposed. VU4**,** VU5, VU6 crop out in the Venetico Marina quarries (sections B and C of Fig. 1), east of the Torregrotta cemetery (Section E of Fig. 2) and between Acquasanta and Scarano localities (sections I and L of Fig. 2). Furthermore, VU5 also occurs on the eastern side of the hill, where the Tracoccìa Village is located (section D of Fig. 2). VU6 is also exposed in the northern boundary of the studied area (section A of Fig. 2), near the margin of the Venetico Marina coastal plain. VU7 is the most widespread among the analysed layers and is found throughout the investigated area, with the exception of Scarano Locality (section L of Fig. 2), where the uppermost portion of the series is truncated by erosion and subsequent deposition of a Tyrrhenian Terrace. VU8 is at the top of the sequence, and crops out sparsely in the northern (sections B, C, E of Fig. 2), central and southern (sections H and I of Fig. 2) sector zones of the investigated area.

The field characteristics, such as thickness, lateral variations, juvenile and lithic component fractions, of the volcaniclastic units are briefly described below, from bottom to top of the stratigraphic sequence. The standard granulometric classification scheme of Fisher (1961, 1966) for pyroclastic rocks associated with explosive and non-explosive fragmentation processes is used in this study. The term "volcaniclastic" was defined by Fisher (1961, 1966) to denominate all clastic sediments and rocks, regardless of depositional process, composed of particles predominantly of volcanic origin.

VU1 (Fig. 3a and b) is lentiform, variably thick (3÷10 cm) and discontinuously outcrops. The basal contact with clays is sharp, from planar to gently undulated. The upper contact is less defined, variously corrugated and sometimes marked by an orange alteration aureole. The textural features allow us to recognize two lithofacies (VU1-1 and VU1-2). The lower one (VU1-1; 1÷2 cm thick; Fig. 3b) is characterized by mm-sized laminae of coarse ash black lithic clasts with massive structure. Some interfingered plane-parallel laminated layers of poorly cemented, well sorted and rounded grey lapilli pumices, are also observed. This lithofacies is characterized by lateral pinch-out closures showing sharp contacts with the upper lithofacies VU1-2. This last lithofacies (VU1-2; Fig. 3b) is composed of clast-supported normal graded slightly cemented grey, mainly sub-rounded pumice lapilli clasts (up to 2–3 cm in diameter), sometimes altered.

VU2 (Fig. 3c and d) shows variable thickness (2.5÷6 cm) with spatial extent up to twenty metres in length, strongly discontinuous and with pocket-like geometry. Generally, it occurs as boudins laterally tapered due to load pressure. Its basal and upper contacts are sharp and irregular and marked by a yellow-orange alteration crust (2÷3 mm thick; Fig. 3d). Evident fluidification structures are observed along the basal surface (Fig. 3d). Generally, this volcaniclastic unit is characterized by a massive appearance (2.5÷4.5 cm thick) composed of prevailing whitish well sorted rounded pumices with subordinate black lithic fragments (1÷3 mm) (Fig. 3d). Locally, especially in the section L (Fig. 1), this volcaniclastic unit is overlain by a layer of clast-supported fine lapilli-sized rounded pumices (2-3 cm thick), through a sharp and gently undulated contact (Fig. 3c).

VU3 is strongly discontinuous, up to 3 cm in thickness, with laminated structure composed of a loose grey fine to medium ash mixed with abundant fine terrigenous sand (mica and quartz), foraminiferal microfauna and minute bioclasts. The basal contact is sharp and slightly undulated; the upper contact is erosive and irregular.

VU4 (Fig. 3e and f) is 5÷18 cm thick and shows a lateral continuity at the scale of outcrop (about 40 m) with general lenticular geometry. Its basal contact with clays is erosive and rather wavy (≈25 cm wavelength), the upper contact is sharp, from planar to slightly wavy sometimes showing load structures (Fig. 3e). This volcaniclastic unit is well exposed in sections L and B (Fig. 1), where two lithofacies have been recognized (VU4-1 and VU4-2; Fig. 3f). The lower VU4-1 subunit is massive, up to 5.5 cm in thickness (section L) and composed of sub-angular and sub-rounded loose black lapilli scoria (2÷3 mm in diameter), sometimes altered and characterized by pinch-out closures (Fig. 3e). The upper subunit (VU4-2) consists of medium-coarse grained ashes, up to 8÷10 cm thick, with distinctive plane-parallel or slightly undulated lamination structures, a few mm in thickness. These structures are marked by alternating light non-volcanic fraction (terrigenous clasts, foraminiferal microfauna and minute bio-clasts) and dark scoria fragments. It is to be emphasized that in the north (Section B) the VU4-1 lithofacies is poorly represented.

VU5 (Fig. 3g) is generally continuous, variably thick (3÷20 cm in the different sections), and shows evident lenticular and pocket-like geometry, on the metre scale (section E). The basal contact with clays is erosive and sharp, showing from slightly to densely wavy channel-like structures, whereas the upper contact is irregular with small steps. Both contacts are often highlighted by an about 1 cm thick orange alteration level (Fig. 3g). The volcaniclastic unit is generally characterized by cm-thick layers (up to three) of structureless to normally graded whitish fine lapilli pumices

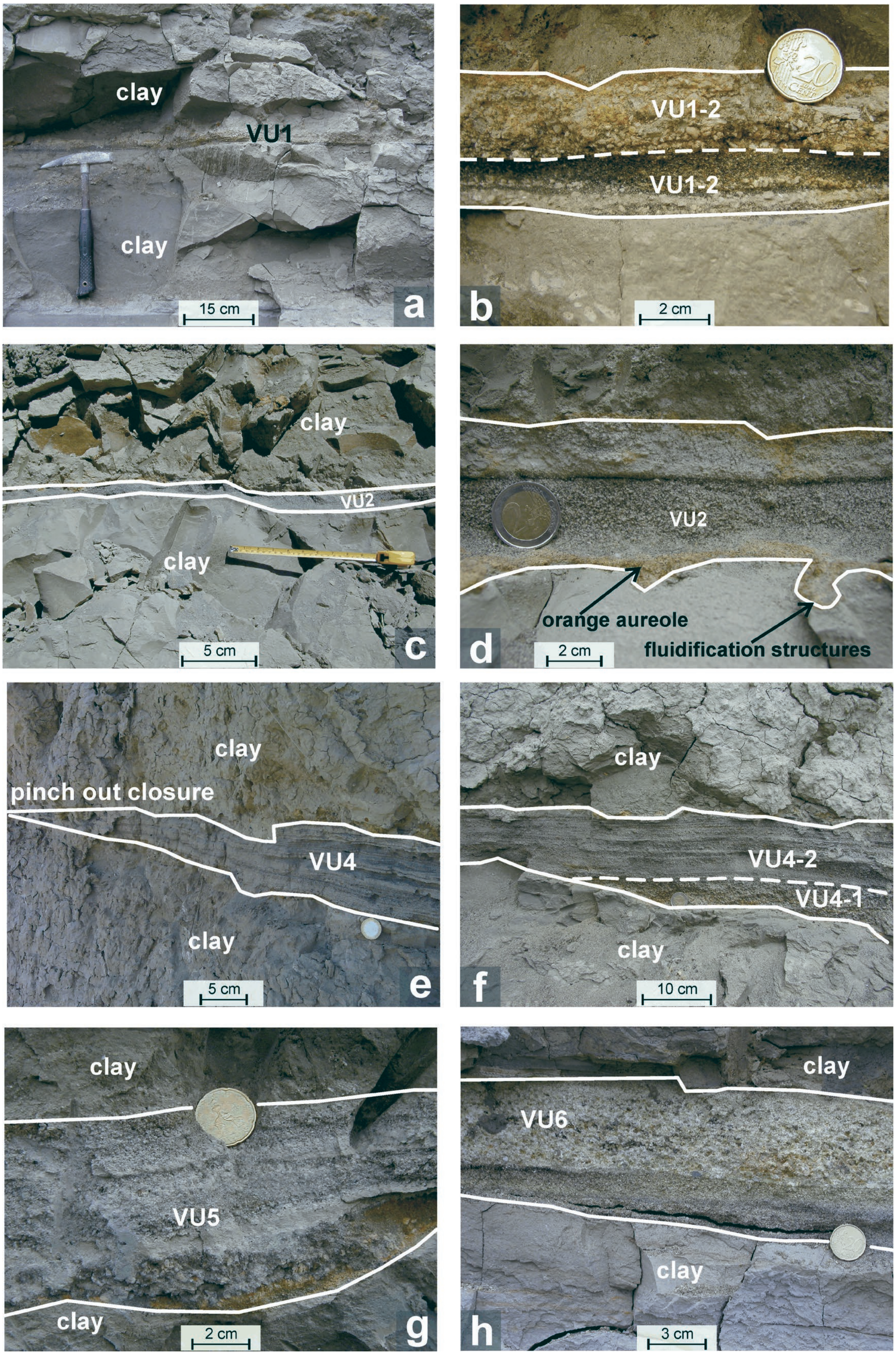

Fig. 3. Outcrop and/or detail photographs of the most representative studied volcaniclastic units: **a, b** — VU1, section B; **c, d** — VU2, section L; **e, f** — VU4, section B; **g** — VU5, section E; **h** — VU6, section I. The white continuous lines indicate the entire volcaniclastic units, the white dashed lines indicate the subunits. See text for details of descriptions.

(up to 1 cm) with rare dark lithic fragments, separated by thin (few mm to 1 cm) intercalations (usually two) of fine grained greyish ash showing erosive contacts (Fig. 3g). The pumice lapilli layers are well sorted and consist of sub-angular and sub-rounded frequently altered clasts. The lowest pumice layer is the coarsest with low matrix fraction and grainy appearance. This layered sequence sometimes starts with lenses (up to 1 cm thick) consisting of prevalent structureless coarse ash (1–2 mm) to whitish pumiceous lapilli.

VU6 (Fig. 3h) shows variable thickness with an average value of 25÷30 cm (~5 cm in section L, ~40 cm in section I) and is laterally continuous with ribbon-like geometry (Hornung et al. 2002). The contact with marly clays is clear and defined by narrow undulations, barely defined at the base and more prominent at the top. In general, the volcaniclastic unit is characterized by an abundant non-volcaniclastic fraction consisting of terrigenous component, Foraminifera (Orbulinidae) and minute bio-clastic fragments mixed with the volcanic fraction mainly consisting of scoria (2÷5 mm). The two fractions are organized in structureless cm-thick layers sometimes with slightly undulated plane-parallel and subordinate low-angle cross lamination. In section L the two layers are distinctively separated by a sharp surface, planar to gently undulated. The latter is composed of terrigenous sediments plus minor scoriae whereas the upper layer is mainly composed of altered yellowish-white pumices (2÷7 mm) with subordinate scoriae (Fig. 3h).

VU7 is the most widely occurring volcaniclastic unit. It is continuous and shows a thickness from a few dm (sections D, E and H) to over 2 m (~2.30 m in section G). Its geometrics generally range from ribbon-like, to channel-shape or gently bell-shaped on the outcrop scale. In Section O thickness variations with reduction up to pinch-out closures have been observed. The basal contact with clays is sharp and slightly wavy to planar; the upper contact is also sharp (Fig. 4a and b). Abruptly truncated erosive lateral closures are observed between sections E and G. In the most complete sequence (sections A, G and N) the VU7 unit shows peculiar lithological and sedimentological features that clearly allow us to define three lithofacies (section G). The lowest lithofacies (VU7-1, Fig. 4c) is informally called the "lithic rich lithofacies" (from 2÷4 cm to >10 cm thick in sections N, A; ~30 cm in section G). It contains abundant black angular lithic clasts (up to 5 cm) mixed with sub-angular/sub-rounded pumices (0.5 cm up to 6 cm), lithified, clast-supported massive structure which locally shows lateral transitions to reverse grading of coarser lapilli (up to 6 cm in section G) (Fig. 4c) with laminated lithic-rich beds (up to 1 cm in section A). Near section E, at the contact surface with the marl-clay substrate, flute-cast structures (N200W–N20E preferential direction) have been identified. The VU7-2 is a planar to cross bedded ash-lapilli tuff lithofacies showing a thickness of ~10÷15 cm reaching 35 cm in section G. Two sub-lithofacies have been recognized (Fig. 4c). Both are well sorted. The lower VU7-2a is more continuous (over 30–50 m) showing prevalent structureless plane-parallel laminae sometimes slightly wavy, with generally regular contacts; the upper sub-lithofacies (VU7-2b) is characterized by mm to cm thick gently wavy with low- to medium-angle cross beds, variously interfingered with very fine-grained whitish pumices and dark lithics. Only in section N, along strata interfaces, the presence of several flute casts with ESE–WNW preferential orientation (N285E) from East-Southeastern to West-Northwestern, marked by orange aureoles (Fig. 4d), was observed. "Tool marks" have also been found. The chromatic variability led us to informally call this sub-lithofacies "Zebra layer" (Fig. 4c).

The third lithofacies (VU7-3, 25–30 cm thick; Fig. 4e) is characterized by the presence of abundant sub-angular to sub-rounded white lapilli pumices, with subordinate randomly dispersed coarse angular lithics (1–2 cm up to 10 cm; Fig. 4f). This lithofacies, informally called "White lapilli pumices", crops out in all the recognized sections representing 60–100 % of the whole VU7. The common presence of at least three erosive contacts, usually marked by cm-thick beds (2–3 cm thick) enriched in mm-sized angular lithics, allow subdivision of the VU7-3 into four sub-lithofacies (Fig. 4e). The lowermost one (VU7-3a) is incised into the underlying VU7-2 with sharp and wavy erosive contact. It is characterized by medium to coarse lapilli with rare dark random lithics, showing the coarser fraction (1–2 cm in size) concentrated in the median portion. VU7-3b (15–100 cm thick), VU7-3c (15–40 cm thick) and VU7-3d (dm–cm thick) show similar compositions to the previous sub-lithofacies but different structures. In particular, VU7-3b is massive (e.g. in section M) with some plane parallel lamination (e.g. in section N, Fig. 4e); VU7-3c is massive and composed of very coarse lapilli (3–6 cm sized) and randomly dispersed sub-rounded to rounded pumiceous clasts (8–12 cm-sized); VU7-3d is normally graded with pumice lapilli (mm-sized) grading upward to whitish fine ash beds (1–8 cm thick) which sometimes display convoluted structures (Fig. 4e).

The sequence described above is frequently incomplete showing stratigraphic gaps and lateral variations, which are continuous on metre-scale but discontinuous over 10's of m (20–30 m). For these reasons, in Fig. 5 a synthetic lithological column is reported relative to the complete sequence of VU7.

The average thickness of VU8 ranges between 10÷15 cm, with a maximum thickness of ~40 cm in section C, and it is widely distributed. Sideways, it is rather continuous with plane-concave lentiform geometry and pinch-out closures. Its basal contact with clays is slightly undulated, the upper erosive contact is markedly undulated and articulated, with small steps. Both contacts are sharp and frequently marked by an orange alteration level (up to 1 cm in size). The unit shows abundant pumices mainly fine-grained (<1 cm in size), loose and sub-rounded and rarely coarse-grained (3–5 cm in size), which are arranged in cm-thick laminae (1–3 cm). The latter are plane-parallel and marked by grey to yellow-orange chromatic variations. Rare dispersed dark lithics have also been found. The pumiceous beds are

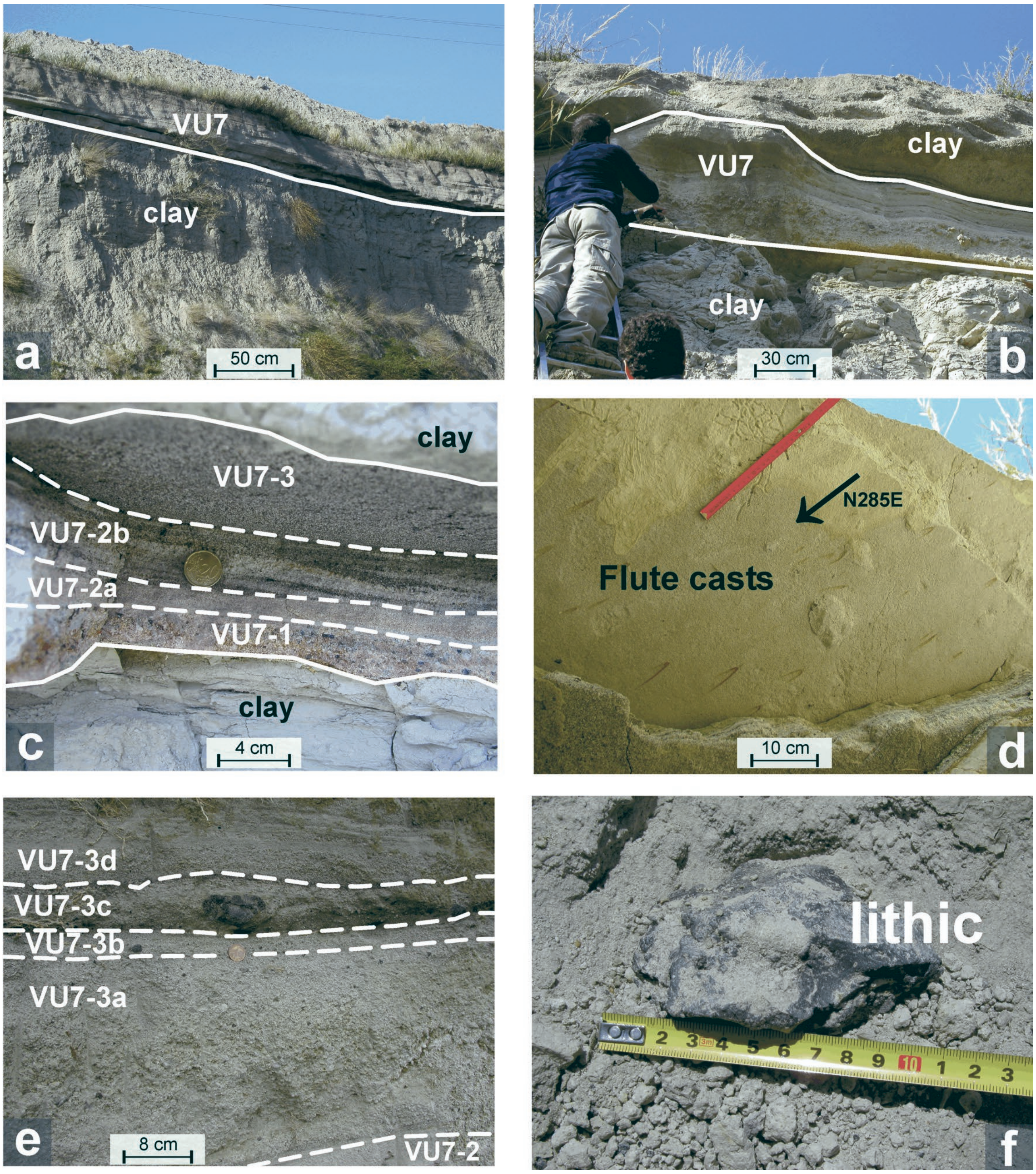

Fig. 4. Representative pictures of structures and detailed features of the VU7 unit: **a, b** — outcrop views, section G; **c** — basal portion, section G; **d** — fingerprints of flute casts with orientation, section N; **e** — middle part, section G; **f** — detail with a sub-angular lithic clast. The white continuous lines indicate the entire volcaniclastic units, the white dashed lines indicate the subunits. See text for details of descriptions.

usually interbedded with mm-sized light grey fine-ashes, which are characterized by slightly wavy erosional surfaces.

Grain size distribution and morphological features of volcanic clasts

The parameters of grain size distribution and summary of volcaniclastic component sorting (Cas and Wright, 1987) are reported in Table 1. The results highlight that VU1, VU5, VU6 and VU8 are well-sorted, VU2, VU3 and VU4 are distinctively uni-modal and better sorted, whereas only VU7-1 and VU7-3 are poorly sorted and show low Mdϕ typical of pyroclastic flow deposits (Table 1).

Representative SEM images of clast morphologies are displayed in Fig. 6. The studied juvenile material shows two main morphologies (Table 2). Some pumice clasts have a fluidal texture with thin, commonly tubular, frequently coalescing vesicles, related to high energy magmatic eruptions (Fig. 6A, C, F, G, H). Other fragments are blocky

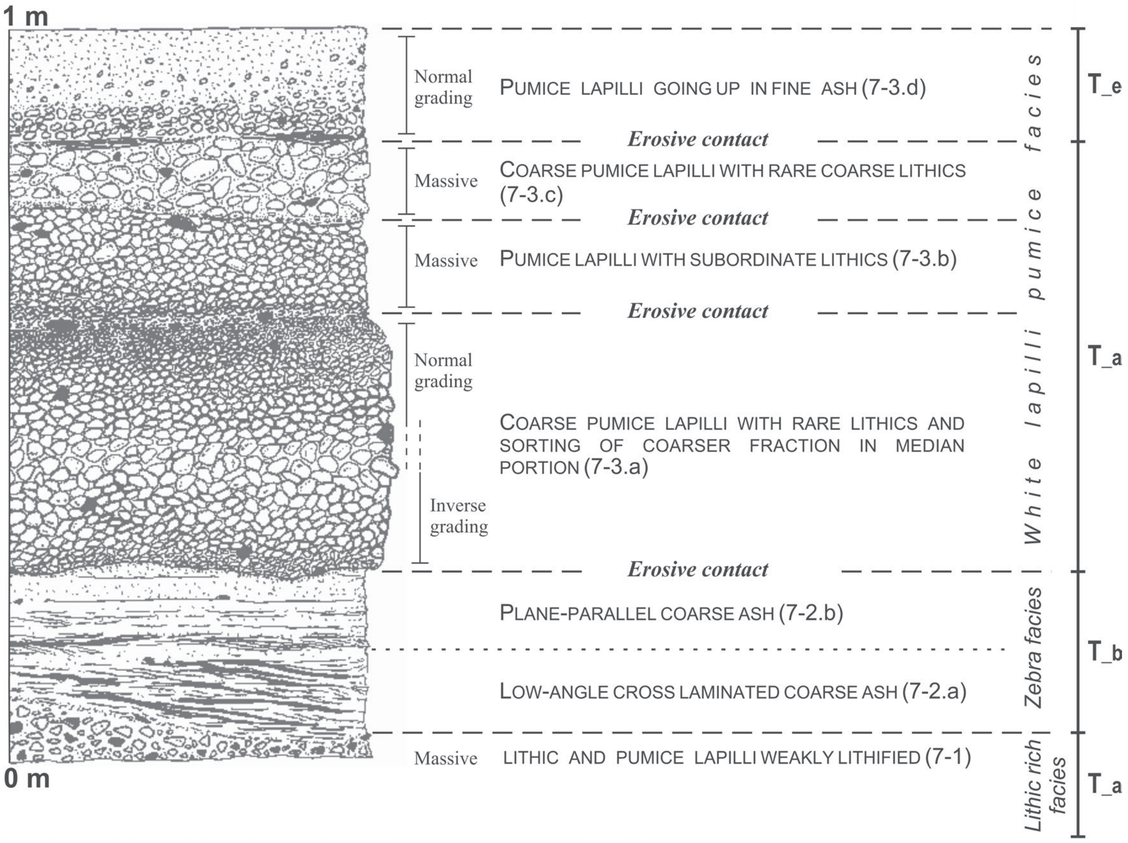

Fig. 5. Reconstructed schematic depositional features of volcaniclastic unit VU7. See text for explanation of emplacement mechanisms.

Table 1: Grain size distribution of representative volcanic component of the studied volcaniclastic units.

Volcaniclastic Units	Mdφ	σφ	Skewness	Sorting*
VU1	0.50	1.40	0.64	Well sorted
VU2	1.60	0.85	0.06	Very well sorted
VU4	-0.65	0.45	0.22	Very well sorted
VU5	1.50	1.55	-0.61	Well sorted
VU7-1	1.60	1.30	0.076	Well sorted
VU7-2	1.00	2.82	0.061	Poorly sorted
VU7-3.1	2.80	1.40	0.14	Well sorted
VU7-3.2	0.20	2.00	0.90	Poorly sorted
VU7-3.3	1.60	1.82	0.31	Well sorted
VU7-3.4	1.55	1.70	0.60	Well sorted
VU8	1.20	1.65	-0.090	Well sorted

(* from Cas & Wright 1987)

and dense poorly vesiculated to massive glassy with conchoidal fracture (Fig. 6D) In both cases, the clasts frequently show surfaces coated with adhering particles (Fig. 6A, C, D, G, H).

Petrography and mineral chemistry

The studied volcaniclastic units are composed of predominant pumices (vesiculated juvenile materials) associated with rare volcanogenic minerals (loose pyroxene and plagioclase crystals) and a basaltic lithic fraction. The results of petrographic and mineral chemistry investigations indicate homogeneous features of the pumice clasts among the various volcaniclastic units in terms of both texture and composition. In general, the various units are characterized by different amounts of non-volcanic extra-basinal and intra-basinal clastic components. Commonly, the extra-basinal fraction, derived from inland, is represented by non-volcanic mineral clasts of quartz, feldspar, chlorite, mica flakes (biotite, muscovite), and fragments of metamorphic, intrusive and sedimentary rocks. The intra-basinal component is represented by clay containing fossils and diffuse pyrite grains.

Juvenile volcanic clasts in all units consist of predominantly white and minor brown pumices, marked by fluidal, spongy and minor blocky texture. The lithic volcanic fraction is mainly represented by rock fragments. Some mafic lithics contain phenocrysts of plagioclase and pyroxene in a groundmass consisting of the same phases plus magnetite and brown glass. Under the microscope most of the lithic clasts show the same mineral assemblage occurring as phenocrysts in pumices, suggesting that they should be considered genetically related to pumices, at least for those contained in the VU7.

Igneous minerals, include plagioclase, clino- and orthopyroxene (Fig. 7A and B). They occur as loose crystals and as phenocrysts in pumices and in lithic clasts of all the volcaniclastic units. Plagioclase appears as the dominant and ubiquitous phenocryst phase as sub-euhedral slightly zoned crystals

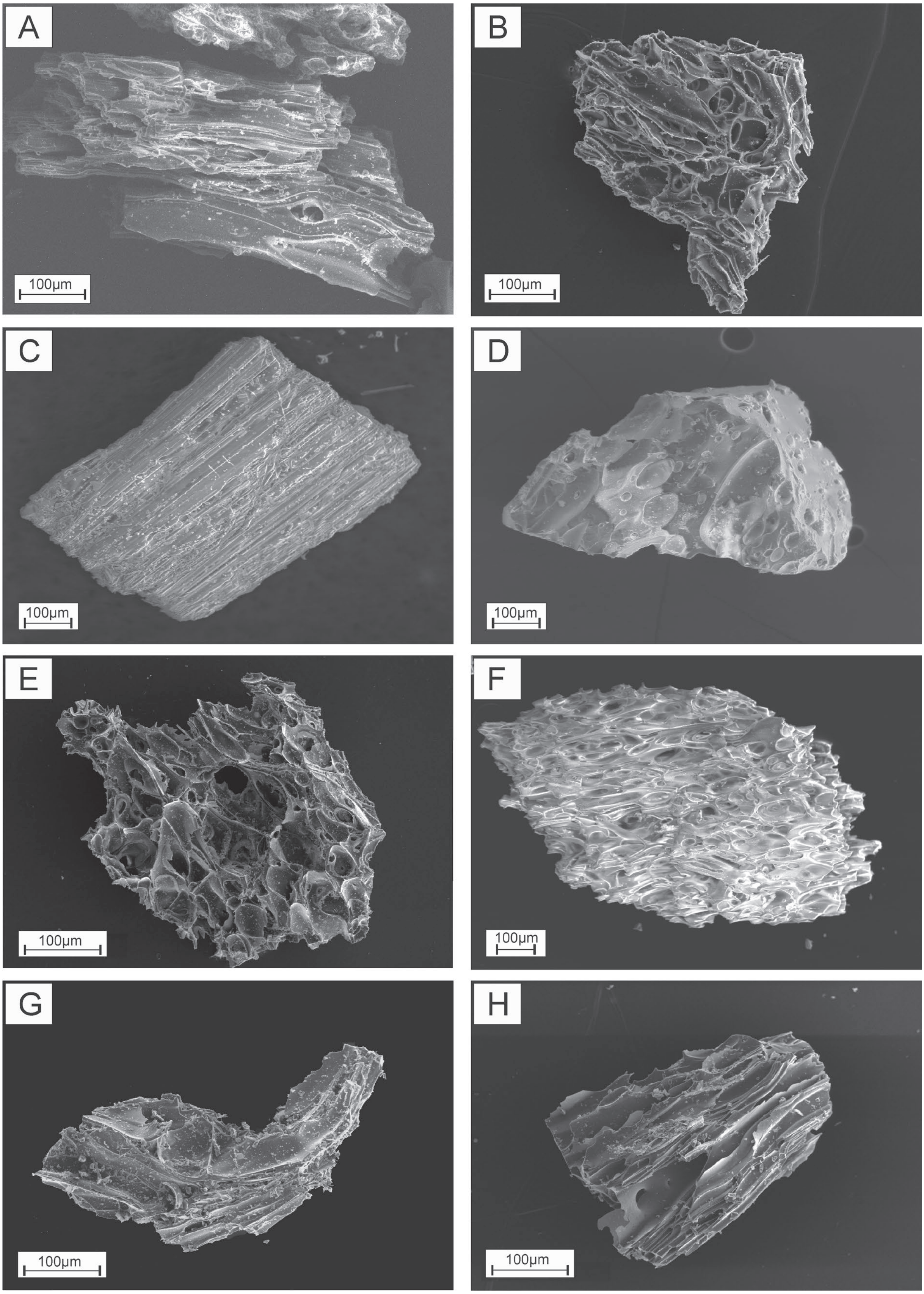

Fig. 6. Secondary electron images of selected pumice grains: **A** — fluidal pumice shards of VU1; **B** — spiny shape of a pumice from VU2; **C** — fluidal and angular shape of a VU3 fragments; **D** — blocky glass grains from VU4; **E** — spiny shape of a VU5 pumice clast; **F** — fluidal pumice fragments from VU6; **G** and **H** — fluidal pumice shards from VU7 and VU8, respectively.

with marked resorption phenomena and frequent inclusions of brown glass. The composition of the analysed plagioclase crystals ranges from andesite to labradorite from rim to core, with average values of An 38÷57 (Fig. 7A). Pyroxene is present as euhedral to subhedral colourless to light-green crystals in all the investigated pumices. Compositions are pigeonite-augite with an average composition of $En_{43}Fe_{18}Wo_{39}$ (Fig. 7B). The orthopyroxene is enstatite (Fig. 7B).

Bulk rock chemistry

Pumice clasts, mainly belonging to the most representative volcaniclastic unit (VU7), have been analysed for major and trace elements. The analytical results are reported in Table 3 (major elements) and Table 4 (trace elements). Most of the samples show high LOI values (> 2.5 %, Table 3), probably due either to primary water and alteration. As alteration may have changed the pristine compositions, especially in terms of alkali contents, the discussion is mainly based on Zr, Y, Nb and Ti considered as immobile trace elements during secondary processes.

The total alkali versus silica (TAS) diagram recalculated on a water-free basis (Le Bas et al. 1986; Fig. 8A) shows subalkaline dacitic and rhyolitic compositions (Fig. 8A) with two samples (VU7.4, VU8) characterized by a slight alkali enrichment, falling in the trachyte field (Fig. 8A). Fig. 8B shows how most of the samples plot in the high potassic calc-alkaline field (Peccerillo & Taylor 1976).

The incompatible trace-element abundances are displayed on the multi-element mantle-normalized diagram (Sun & McDonough 1989; Fig. 8C), in which the negative Nb anomaly and the positive Pb spike are evident. On the Ti-Zr-Y tectonic discrimination diagram (Pearce & Cann 1973) all the samples fall in the field of volcanic arc products (Fig. 8D).

Discussion

Emplacement mechanisms

The eight volcaniclastic units besides other ten minor lens-shaped discontinuous volcaniclastic horizons (up to 3 cm thick) generally composed of ash to very-fine whitish pumiceous lapilli and ranging in age from 980–910 ka to 589 ka (Castradori 1993; Sprovieri et al. 1998, Cita et al. 1998), provide compelling evidence for an intense long-lasting volcanic activity with variable composition of the erupted products. Clasts have settled in a subaqueous environment to a depth of about 500–700 metres, in an upper epi-bathyal zone, as suggested by the constant presence of a benthic fossil association (Violanti, 1989).

Field investigations suggest that all the studied volcaniclastic units are well correlated for all the thirteen examined stratigraphic sections (Figs. 1 and 2) as indicated by the same mutual stratigraphic position, by the comparable thicknesses

Table 2: Morphologies of the analyzed juvenile clasts.

Samples	Clast morphologies	Description
VU1	Fluidal pumice	Well vesiculated, surfaces coated with fine adhering particles.
VU2	Blocky	Higly vesiculated, elongated to sub-spherical bubbles, conchoidal surfaces coated with fine adhering particles, trace of mechanical modifications due to transport.
VU3	Fluidal angular shape pumice	Strongly stretched vesicles, slight coated with fine adhering particles.
VU4	Blocky	Moderately vesiculated, sub-spherical and elongated vesicles with thick walls, trace of modifications by mechanical abrasion.
VU5	Blocky glass	Highly vesiculated, sub-spherical to elongated vesicles with thin walls, surfaces coated with fine adhering particles.
VU6	Fluidal pumice	Spiny shaped with sub-spherical to elongated vesicles.
VU7	Fluidal pumice and blocky	Fluidal shaped with tubular large and small vesicles, evidence of stretching effects - blocky shaped, pits due to chemical etching – on both types surfaces coated with fine adhering particles and no signs of surface modifications due to transport processes.
VU8	Fluidal pumice	Parallel elongated vesicles with tiny walls, surfaces coated with fine adhering particles.

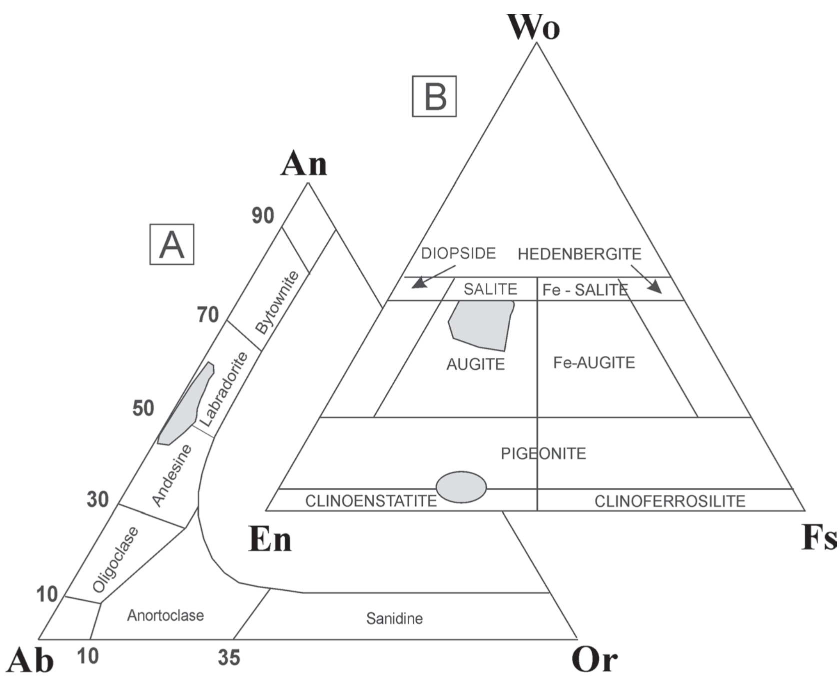

Fig. 7. Composition domains (grey) of plagioclase (**A**) and pyroxene (**B**) of the samples from the studied volcaniclastic units.

Table 3: XRF major elements data of the analyzed pumice clasts from the volcaniclastic units.

SAMPLES		SiO_2	TiO_2	Al_2O_3	Fe_2O_3	FeO	MnO	MgO	CaO	Na_2O	K_2O	P_2O_5	LOI
		weight %											
VU1	*white pumice*	62.11	0.85	13.96	3.29	3.48	0.16	1.25	3.47	3.78	2.73	0.18	4.72
VU2	*white pumice*	67.36	0.57	12.36	1.96	2.53	0.13	0.53	1.82	4.06	3.29	0.06	5.33
VU4-1	*dark pumice*	58.19	1.09	13.97	5.19	5.46	0.18	2.52	5.48	3.31	2.13	0.19	2.29
VU4-2	*dark pumice*	58.26	1.15	14.13	4.46	5.98	0.18	2.55	5.65	3.31	2.22	0.18	1.92
VU5-1	*white pumice*	65.29	0.58	12.35	3.41	2.90	0.16	0.65	2.53	3.85	3.51	0.12	4.65
VU5-2	*white pumice*	63.84	0.54	13.37	4.69	1.96	0.14	0.69	2.39	3.84	3.07	0.10	5.38
VU7-1	*white pumice*	68.39	0.67	14.48	2.70	1.79	0.15	0.94	2.72	4.47	2.98	0.14	0.55
VU7-2	*white pumice*	66.42	0.69	13.77	2.26	1.82	0.15	0.90	2.63	4.12	3.15	0.12	3.98
VU7-3	*dark pumice*	62.05	0.92	13.95	4.10	3.95	0.18	1.78	4.71	3.86	2.42	0.21	1.87
VU7-4	*white pumice*	61.11	1.25	9.70	7.14	2.07	0.30	0.83	4.42	3.97	4.62	0.14	4.44
VU7-5	*white pumice*	66.30	0.71	13.73	1.99	2.31	0.15	0.88	2.32	3.96	2.70	0.10	4.86
VU7-6	*white pumice*	68.96	0.81	12.10	2.80	2.38	0.16	0.90	2.88	4.25	3.05	0.09	1.61
VU7-7	*white pumice*	66.80	0.69	13.38	1.75	2.48	0.15	0.83	2.42	4.00	2.91	0.11	4.48
VU7-8	*white pumice*	65.89	0.69	13.32	1.88	2.30	0.14	1.07	2.53	3.98	2.93	0.11	5.18
VU7-9	*white pumice*	66.28	0.72	13.46	2.30	2.19	0.17	0.79	2.29	3.92	2.97	0.11	4.80
VU7-10	*dark pumice*	67.17	0.70	13.38	1.74	2.26	0.14	0.82	2.38	3.93	3.16	0.11	4.21
VU7-11	*white pumice*	67.83	0.74	14.44	2.59	2.12	0.16	0.88	2.79	4.33	3.02	0.15	0.97
VU7-12	*white pumice*	67.62	0.67	13.24	1.67	2.26	0.14	0.83	2.23	3.80	2.85	0.10	4.60
VU7-13	*white pumice*	68.23	0.67	12.66	2.10	1.86	0.13	0.90	2.34	3.79	2.74	0.11	4.47
VU7-14	*white pumice*	64.11	0.74	13.54	4.42	1.93	0.13	1.03	3.41	3.61	2.38	0.14	4.57
VU8-1	*white pumice*	63.21	0.97	9.81	5.79	2.11	0.23	0.69	3.55	3.88	4.39	0.10	5.28

Table 4: XRF trace elements data of the analyzed pumice clasts from the volcaniclastic units.

SAMPLES		V	Cr	Co	Ni	Cu	Zn	Ga	Rb	Sr	Y	Zr	Nb	Ba	La	Pb	Ce	Th
		ppm																
VU1	*white pumice*	44	7	9	6	10	99	22	80	384	36	170	10	572	32	21	73	9
VU2	*white pumice*	13	7	1	10	9	76	20	97	280	36	197	11	670	31	24	62	17
VU4-1	*dark pumice*	272	20	24	19	42	107	24	71	429	29	146	12	473	27	19	65	8
VU4-2	*dark pumice*	322	24	22	11	39	100	24	70	447	31	150	11	494	29	14	47	6
VU5-1	*white pumice*	6	7	3	11	13	101	32	106	293	33	198	10	644	40	41	86	27
VU5-2	*white pumice*	10	3	1	15	17	90	20	96	315	38	189	11	624	33	20	131	19
VU7-1	*white pumice*	24	7	5	12	7	79	19	88	383	31	186	13	660	42	17	66	10
VU7-2	*white pumice*	21	6	5	11	7	81	17	92	361	31	184	12	646	42	17	70	10
VU7-3	*dark pumice*	125	16	8	12	16	96	22	73	466	27	154	11	521	38	17	104	6
VU7-4	*white pumice*	15	7	5	11	26	127	41	114	447	46	226	14	606	40	52	70	37
VU7-5	*white pumice*	15	4	6	8	11	95	20	85	364	32	182	11	718	36	27	69	16
VU7-6	*white pumice*	24	6	4	13	11	97	23	92	379	35	181	10	610	33	25	58	22
VU7-7	*white pumice*	19	5	3	10	10	79	17	83	350	37	182	11	635	40	22	60	16
VU7-8	*white pumice*	18	5	3	8	8	79	17	82	362	36	183	11	634	37	21	69	15
VU7-9	*white pumice*	15	3	4	10	12	86	24	90	332	35	178	10	623	35	31	68	24
VU7-10	*dark pumice*	15	6	2	10	10	85	21	89	346	33	173	10	641	36	25	64	25
VU7-11	*white pumice*	21	6	3	12	10	85	20	90	379	33	183	11	662	39	20	61	15
VU7-12	*white pumice*	16	5	1	9	8	83	17	81	347	36	182	11	662	38	23	71	14
VU7-13	*white pumice*	24	9	1	6	9	83	24	80	341	34	163	9	633	40	33	65	21
VU7-14	*white pumice*	52	6	9	17	14	74	23	74	320	27	161	9	519	21	26	90	15
VU8-1	*white pumice*	16	6	7	18	348	100	34	116	371	36	217	12	593	37	41	87	23

of the neighbouring clays, by the uniformity of their sedimentological and petrographic features. Each volcaniclastic unit, correlated in various sites, belongs to the same depositional event and therefore to the same eruptive or post-eruptive phase.

In most cases the units are composed of whitish pumiceous lapilli with variable amounts of admixed lithic clasts, except for the VU4 which is composed of prevailing black lapilli to ash-sized scoriae. Among the units, VU7 is the most prominent for its thickness of about 1 to 2.3 metres, the lateral extension and also for its occurrence over a wide area. Sedimentological features allow us to subdivide some volcaniclastic units into distinct lithofacies. The VU3, VU4 and VU6 units contain abundant exotic terrigenous clasts, foraminiferal microfauna and minute bio-clasts mixed with volcaniclastic materials. Because of the presence of basal scouring and their internal structures indicative of water-supported gravitational flows, these are interpreted as epiclastic units. They were generated by re-depositional processes and are defined as secondary volcaniclastic products related to post-eruptive processes. Contrastingly, the non-contaminated volcaniclastic units (VU1, VU2, VU5, VU7, VU8),

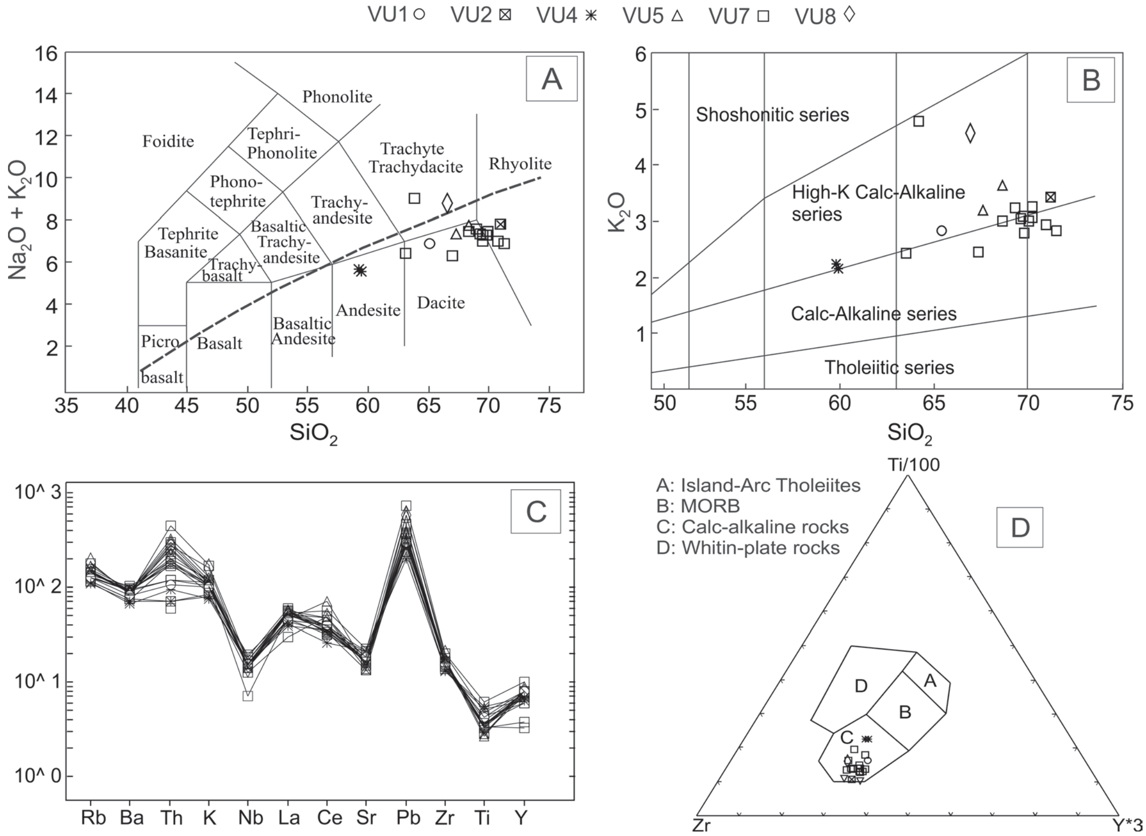

Fig. 8. Major and trace elements composition diagrams of the analyzed pumice clasts [VU7 has also lithic clasts, not only pumice!] from the studied volcaniclastic units. **A** — TAS classification diagram of Le Bas et al. (1986); **B** — SiO_2 vs K_2O classification diagram of Peccerillo & Taylor (1976); **C** — Spider diagram of incompatible elements normalized to primordial mantle composition (McDonough et al. 1992); **D** — Tectonic classification diagram based on HFS elements (after Pearce & Cann 1973).

consisting entirely of fresh volcanic fragments, are regarded as primary deposits originated by subaqueous concentrated density flows (Mulder and Alexander, 2001).

Density currents bearing unmodified eruption-formed fragments originate either directly from volcanic eruptions (pyroclastic flows) or indirectly by remobilization and redeposition of material initially emplaced by a different process (Fisher & Schmincke 1984; Cas & Wright 1987; McPhie et al. 1993). For submarine settings, even deposits formed by pyroclastic fragmentation followed by uninterrupted transport through the ambient water column have been commonly termed as reworked or redeposited (Cas & Wright 1987; McPhie et al. 1993). Consequently, remobilized unconsolidated pyroclastic debris transported downstream via density current processes in a submarine setting with preserved pyroclastic components may be referred to as pyroclastic in origin. Pumice shreds, vitric shards, broken or euhedral crystals, and vesicular to non-vesicular, angular lithic fragments (Fisher & Schmincke 1984; Stix 1991) are consistent with a pyroclastic origin as a direct result of volcanic activity.

The compositional homogeneity of the volcanic products and the absence of interbedded clayey layers suggest that deposition occurred almost contemporary with the eruption phases, quickly enough to inhibit the resumption of normal marine sedimentation before volcanic activity ceased. Therefore, the VU1÷VU8 volcaniclastic units are considered cold mass flow deposits as the direct result of an eruption, with transport and deposition mechanism controlled by aqueous processes. VU7 best illustrates the primary pyroclastic origin of these deposits. The flute casts in the plane-parallel laminated facies (VU7-2b), channel scours bedforms, channel-shape geometry of deposits outcrops (Fig. 4) and dip directions of slumpings of VU7 indicates a remobilization of primary pyroclastic material in a near-shore environment, probably outer muddy continental shelf, located to the south-southeast, during or immediately after their primary submarine deposition.

The interaction between volcanism and sedimentation, and the development of concurrent facies are largely governed by two factors: 1) the active volcanism producing abundant material which is rapidly delivered to the deposition sites, and 2) the lateral changes which are the result of flow transformations. During eruptions large volumes of pyroclastic materials are released far more rapidly than any production process of epiclastic particles.

Type of eruptions

The investigated submarine volcaniclastic deposits are diagnostic of different types of eruption. The analysis of the morphological features of juvenile clasts is a valid tool for reconstructing the modalities of magma vesiculation and fragmentation during explosive eruptions (Heiken & Wohletz 1985). In particular, morphological analyses have been performed to infer the style of fragmentation and especially the active involvement of external fluids (phreatic or surface water, steam) in the eruption dynamics (Wohletz 1983; Dellino & La Volpe 1996). Volcanic ash particles from different fragmentation mechanisms have different surface textures and morphologies. The particles forming the analysed volcaniclastic units show mainly pyroclasts with fluidal textures. The predominance of fluidal and highly vesicular fragments over the blocky, dense clasts in the lapilli layers is evidence of pure magmatic fragmentation. The blocky type clasts, are dense fragments frequently marked by conchoidal external surfaces with the presence of adhering particles (Heiken & Wohletz 1985). This is a typical morphology of hydroclastic tephra formation from a system associated with shallow-water phreatomagmatic explosions, in which the explosive vaporization of external water results in the fragmentation and quenching of magma (Heiken & Wohletz 1985, 1991; Wholetz 1987; Houghton & Wilson 1989; Buttner et al. 1999). The angular blocky glassy shards, the presence of glass alteration and the presence of adhering particles on the external surface of the clasts, indicate the important role of magma-water interaction (Wohletz 1983; Sheridan & Wohletz 1983; Kokelaar 1986; Wohletz 1987).

Abundant angular lithic fragments and sub-angular to rounded pumices, both coarser in size, low vesicular to high vesicular pumices, suggest depositional mechanisms as a result of either fallout and pyroclastic flows during moderate Vulcanian to large magnitude Plinian subaerial and/or shallow-water phreatomagmatic eruptions.

The presence of (rare) lithic fragments combined with the estimated volume of VU7 unit exceeding 2×10^6 m^3 (assuming a conservative average thickness of 0.5 m over the whole distribution area) are consistent with partial volcanic conduit collapse and/or vent clearing events during the volcanic eruption.

Provenance of the volcaniclastic deposits

The analysed volcaniclastic-sequence represents the product of explosive volcanic events from one or more volcanic centres located in the Southern Tyrrhenian area. The mineral assemblage, including orthopyroxene phenocrysts, and the geochemical data (especially high ratios of LILE/HFSE) highlight that the studied tephra originated in a volcanic arc environment.

The volcanic centres in the Southern Tyrrhenian Sea characterized by arc signature are the seven subaerial volcanic edifices of the Aeolian islands and the seamounts roughly distributed around the Marsili Basin (Romagnoli 2013; Romagnoli et al. 2013) (Fig. 1). The age of the subaerial Aeolian volcanism ranges from 219 ka (Filicudi) to Present (Stromboli) (De Astis et al. 2003; De Rosa et al. 2003, Peccerillo 2005), younger than the studied volcaniclastic deposits (Lucchi et al. 2013). The oldest documented volcanic activity is represented by the 1.3 Ma age of dredged samples coming from the Sisifo seamount (in the western submarine portion of the arc).

Structural and magmatic variations recognized along the arc depending on the variable composition of the subducted slab (oceanic in the west and oceanic plus sediments in the east), as well as on the local structural setting (e.g. Peccerillo & Frezzotti 2015). On the basis of geochemical and isotopic features, three distinct sectors have been identified in the arc (Calanchi et al. 2002; Peccerillo 2005): 1) the western sector includes the Alicudi and Filicudi islands and consists of calc-alkaline basalt to andesite and minor dacites, characterized by typical island arc signature; 2) the central sector, including Salina, Vulcano, Lipari and Panarea islands, which consists of calc-alkaline to shoshonitic mafic to silicic rocks, with abundant rhyolites mainly erupted during the latest volcanic phases; 3) the eastern sector formed by the Island of Stromboli characterized by calc-alkaline to potassic-alkaline mafic-intermediate rocks showing isotopic incompatible trace element ratios and radiogenic isotope signatures different from those of the western and central islands (Peccerillo et al. 2013).

From the geochemical point of view, the studied volcaniclastic sequence is characterized by arc signature, mostly felsic with subordinate mafic compositions represented by two andesites samples from VU4. Most of the pumices show mainly dacitic and rhyolitic compositions, characterized by CA and HKCA affinity (Fig. 8B), without significant variability inside each unit and among the different units. The volcanic arc signature is indicated by negative anomalies of Nb and Zr and by the positive spike of Pb (Fig. 8C). Trace elements ratios of the most evolved pumices, such as Zr/Nb (17÷21), Rb/Nb (5÷8) and Ba/Rb (5÷8) are slightly variable.

The age of the volcaniclastic sequence and the chemical composition of the studied products suggest that they could be related to the oldest phases of the Aeolian Arc volcanism, effectively excluding an origin from the younger volcanic systems currently exposed above sea-level (De Rosa et al. 2003; Dolfi et al. 2007). Affinity with dacites found within the oldest part of the Panarea volcanic complex dated 800 Ky (Savelli 2002; Lucchi et al. 2013 and references therein) can be considered.

The geochemical data we recorded are compared with those of subaerial volcanic rocks from the Aeolian archipelago (Peccerillo 2005) as well as with the coeval volcaniclastic deposits outcropping along the Calabrian coast (De Rosa et al. 2008). The comparison does not highlight any clear correlation with the CA and HKCA rocks from the

Aeolian islands (Fig. 9) especially regarding the trace elements and their ratios. In contrast, the comparison with data of the coeval Pleistocene tephra outcropping along the Calabrian coast reveals similar Zr/Nb and Ba/Rb ratios. According to De Rosa et al. (2008) it could represent the product of explosive activity from one or more volcanic centres active in the Southern Tyrrhenian domain during the last one million years. Such an eruption centre has been identified in the seamount located 6 miles off the western coast of the Calabria region (Loreto et al. 2015), (Fig. 9).

Combining all the recovered information, it seems very unlikely that the Aeolian Islands are the origin of the studied deposits (VU7, in particular), and difficult to explain the presence of the deposits over the northern Sicilian coast taking into account their distance (> 30 km) and their coarse grain size. The seamount located offshore from the Capo Vaticano promontory (Loreto et al. 2015) looks to be very far away, (about 80 km to the North although compatible in age and chemistry (De Rosa et al. 2008; De Ritis et al. 2010) with the top located at shallow depth (about 70 m b.s.l.). The grain size characteristics of the pyroclastic material of VU7 and also of VU1, VU2, VU5, VU8 indicate a primary emplacement at a distance of less than 5 km from the vent, on a deep shore environment of the Sicilian continental margin, and subsequently remobilization and final redeposition away towards the northwest and north by means of sea currents.

The existence of a subaerial or shallow-water volcanic edifice located somewhere between the northern coast of Sicily, the western coast of Calabria and the Aeolian Islands (Fig. 10) would also be able to explain the abundance of coarse angular lithic and pumiceous clasts (both up to 10–12 cm). This possibility cannot be rejected.

Conclusions

The results of this study highlight for the first time that volcaniclastic deposits outcropping along the Tyrrhenian coastline of the Peloritani Mountains (Sicily) are related to recent (Lower-Middle Pleistocene) explosive activity in the Southern Tyrrhenian sea. The results match those of similar deposits spread over the Mesima-Gioia Tauro and Reggio Calabria basins (De Rosa et al. 2008) for which a possible explosive centre has been identified offshore from the Capo Vaticano promontory (Loreto et al. 2015) while there is no clear correlation with rocks from the subaerial portion of the Aeolian archipelago.

The field investigations besides the sedimentological features of the widespread volcaniclastic deposits suggest that they underwent reworking by sea currents after the primary emplacement. The volcaniclastic units can be identified as the results of deposition of pyroclastic fall and/or flow related to Vulcanian to Plinian type eruptions. Clasts underwent

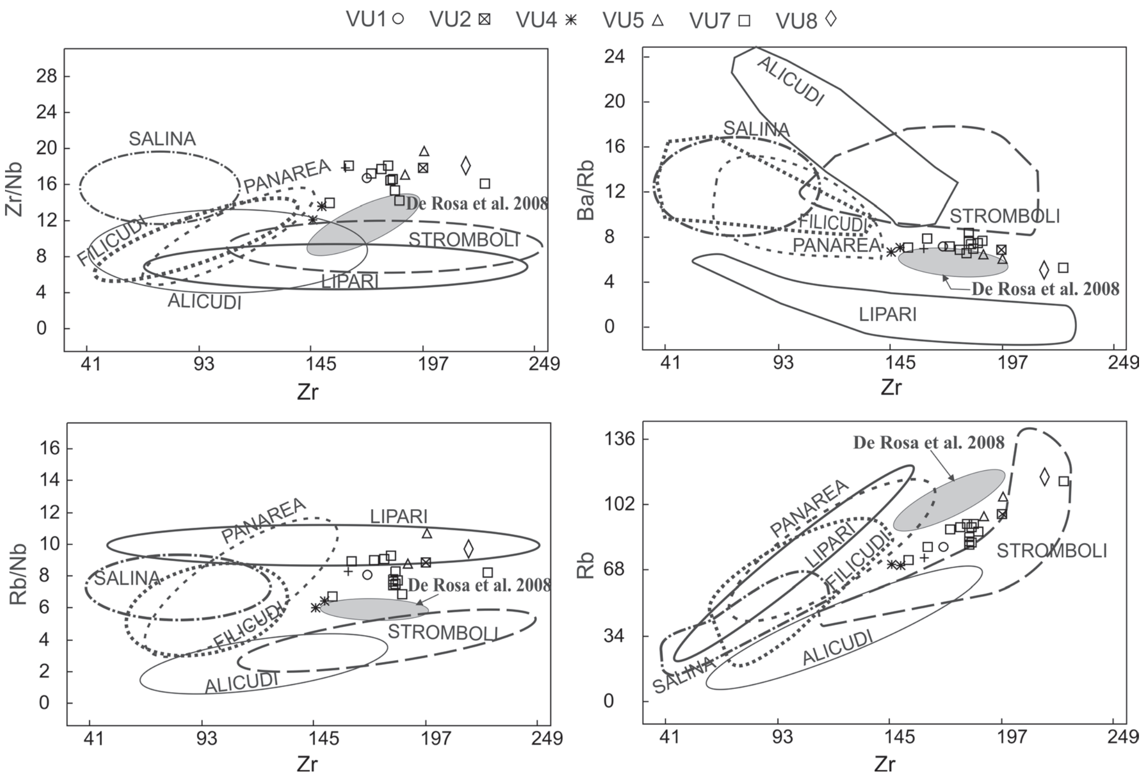

Fig. 9. Rb, Zr/Nb, Ba/Rb and Rb/Nb versus Zr diagrams of analyzed pumice clasts compared with literature data of Aeolian Islands (Peccerillo 2005) and Calabrian volcanic products of similar in age (De Rosa et al. 2008). Symbols are the same as in Fig. 8.

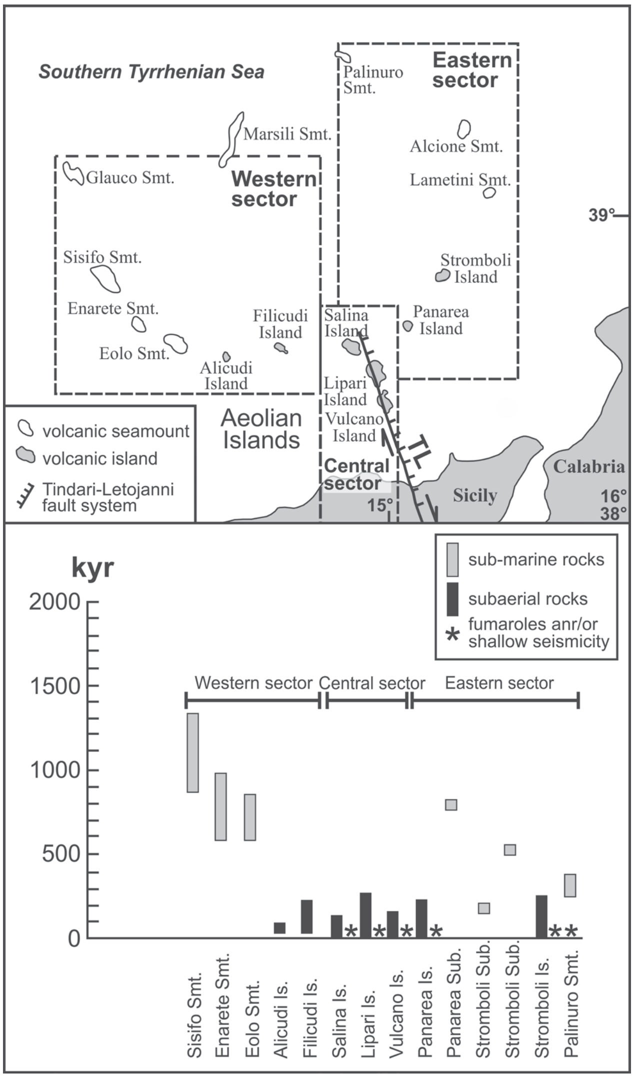

Fig. 10. Structural scheme (above) and summary of available age data showing evolution of volcanism (below) in the Aeolian area (following De Astis et al. 2003, modified).

syn- to post-eruptive remobilization onto the seafloor by density currents. Alternatively, they may represent the extension of subaerial pyroclastic flows entering into the sea and triggering subaqueous dense currents.

The volcaniclastic units probably derive from a common source as testified by a single trend of magmatic differentiation. The presence of the volcaniclastic deposits included in deep water marine clayey sediments allow us to conclude that intense and prolonged explosive mafic to felsic calc-alkaline and high-K calc-alkaline activity occurred at a volcanic centre or centres located in the Southern Tyrrhenian Sea.

Acknowledgements: This paper is dedicated to the memory of our friend, Prof. Riccardo Rasà. The authors are grateful to the 2 anonymous reviewers for their constructive reviews that improved the quality of the paper. They also thank Mauro Coltelli (INGV Catania) for his useful suggestions. The XRF Laboratory of the University of Modena and Reggio Emilia is acknowledged for the technical support during the chemical analyses.

References

Barberi F., Gasparini P., Innocenti F. & Villari L. 1973: Volcanism of the southern Tyrrhenian Sea and its geodynamic implications. *J. Geophys. Res*. 78, 23, 5221–5232.

Barberi F., Civetta L., Gasparini P., Innocenti F., Scandone R. & Villari L. 1974: Evolution of a section of the Africa-Europe plate boundary; paleomagnetic and volcanological evidence from Sicily. *Earth Planet. Sci. Lett.* 22, 2, 123–132.

Barrier P., Cravatte J., Decis R., Lanzafame G. & Ott D’estevou P. 1987: Mise au point stratigraphique sur les relations entre la “couverture calabridemiocene” et les “terrains postorogéniques” dans la region du Detroit de Messine. *IGAL* 11, 43–53.

Beccaluva L., Rossi P.L. & Serri G. 1982: Neogene to Recent volcanism of the Southern Tyrrhenian-Sicilian area: Implications for the geodynamic evolution of the Calabrian Arc. *Earth Evol. Sci.* 3, 222–238.

Beccaluva L., Gabbianelli G., Lucchini F., Rossi P.L. & Savelli C. 1985: Petrology and K/Ar ages of volcanic dredged from the Eolian seamounts: Implications for geodynamic evolution of the Southern Tyhrrenian basin. *Earth Planet. Sci. Lett.* 74, 187–208.

Bigazzi G. & Carobene L. 2004: Dating an ash layer of the Middle Pleistocene: relations to sedimentation, uplift and marine terrace in Crosia-Calopezzati, Calabria (Italy). *Il Quaternario* 17, 2, 151–163. (in Italian with English abstract)

Bonfiglio L. & Violanti D. 1984: First record of Tyrrhenian age and Pleistocenic evolution of Capo Peloro (North-Eastern Sicily). *Geogr. Fis. Dinam. Quater.* 6, 3–15. (in Italian)

Buttner R., Dellino P. & Zimanowsky B. 1999: Identifying magma-water interaction from the surface features of ash particles. *Nature* 401, 6754, 688–690.

Calanchi N. 1988: Quaternary pyroclastic layers in cores from SE sector of the Tyrrhenian Sea: geochemical characters and origins. *Boll. Soc. Geol. It.* 107, 2, 373–382. (in Italian with English abstract).

Calanchi N., Peccerillo A., Tranne C., Lucchini F., Rossi P.M., Kempton P., Barbieri M. & Wu T.W. 2002: Petrology and geochemistry of the island of Panarea: implication for mantle evolution beneath the Aeolian island arc (Southern Tyrrenian Sea, Italy). *J. Volcanol. Geotherm. Res.* 115, 367–395.

Caracausi A., Favara R., Italiano F., Nuccio P.M., Paonita A. & Rizzo A. 2005: Active geodynamics of the central Mediterranean Sea: Tensional tectonic evidences in western Sicily from mantle-derived helium. *Geophys. Res. Lett.* 32, L04312.

Carbone S., Messina A. & Lentini F. 2008: The Geological Map of Italy (Scale 1:50.000) — Sheet 601 Messina–Reggio di Calabria, APAT, Dipartimento Difesa del Suolo. *Servizio Geologia d’Italia*, 1–179.

Carminati E., Lustrino M. & Doglioni C. 2012: Geodynamic evolution of the central and western Mediterranean: Tectonics vs. igneous petrology constraints. *Tectonophysics* 579, 173–192.

Carobene L., Cirrincione R., De Rosa R., Gueli A., Marino S. & Troja O. 2006: Thermal (TL) and optical stimulated luminescence (OSL) techniques for dating Quaternary colluvialvolcaniclastic sediments: an example from the Crati. *Quaternary Internat.* 148, 1, 149–164.

Cas R.A.F. & Wright J.V. 1987: Volcanic Successions: Modern and Ancient. *Unwin Hyman,* London, 1–528.

Castradori D. 1993: Calcareous nannofossil biostratigraphy and biochronology in eastern Mediterranean deep-sea cores. *Rivista Italiana di Paleontologia e Stratigrafia* 99, 107–126.

Catalano S. & Cinque A. 1995: Neotectonic evolution of the northern Peloritani Mountains (NE Sicily): the contribution of a preliminary geomorphological analysis. *Studi Geol. Camerti* 2, 113–123. (in Italian)

Catalano S. & Di Stefano A. 1997: Pleistocene tectonic uplift along the Tyrrhenian margin of the Peloritani Mountains: integration of geomorphological, structural and biostratigraphic data. *Il Quaternario* 10, 2, 337–342. (in Italian with English summary).

Catalano S., De Guidi G., Monaco C., Tortorici G. & Tortorici L. 2003: Long-term behaviour of the late Quaternary normal faults in the Straits of Messina area (Calabrian arc): structural and morphological constraints. *Quaternary Internat.* 101, 81–91.

Cello G., Spadea P., Tortorici L. & Turco E. 1983: Plio-Pleistocene volcanoclastic deposits of southern Calabria. *Boll. Soc. Geol. It.* 102, 87–93.

Cita M.B., Racchetti S., Brambilla R., Bertarini L., Colombaroli D., Morelli L., Negri M., Ritter M., Rovina E., Sala P. & Sanvito S. 1998: Evolution of the deep basins of the Mediterranean recorded by changes in sedimentation rate in the Plio-Pleistocene. *Rend. Fis. Acc. Lincei* 9, 83–100. (in Italian with English abstract).

Cita M.B., Capraro L., Ciaranfi N., Di Stefano E., Marino M., Rio D., Sprovieri R. & Vai G.B. 2006: Calabrian and Ionian: A proposal for the definition of Mediterranean stages for the Lower and Middle Pleistocene. *Episodes* 29, 2, 107–114.

Cornette Y., Gillot P.Y., Barrier P. & Jehenne F. 1987: Donnèsradiometriquès preliminaries (Potassium-Argon) sur des cinèritesplio–plèistocènes du Dètroit de Messine. Doc. et Trav. *IGAL*, 11, 97–99.

Cucci L. 2004: Raised marine terraces in the Northern Calabrian arc (Southern Italy): a 600 kyr-long geological record of regional uplift. *Annals of Geophysics* 47, 4, 1391–1406.

De Astis G., Ventura G. & Vilardo G. 2003: Geodynamic significance of the Aeolian volcanism (Southern Tyrrhenian Sea, Italy) in light of structural, seismological and geochemical data. *Tectonics* 22, 4, 1040–1057.

Dellino P. & La Volpe L. 1996: Image processing analyses in reconstructing fragmentation and transportation mechanism of pyroclastic deposits. The case of monte Pilato-Rocche Rosse Eruptions, Lipari (Aeolian Island, Italy). *J. Volcanol. Geotherm. Res.* 71, 13–29.

De Ritis R., Dominici R., Ventura G., Nicolosi I., Chiappini M., Speranza F., De Rosa R., Donato P. & Sonnino M. 2010: A buried volcano in the Calabrian Arc (Italy) revealed by high resolution aeromagnetic data. *J. Geophys. Res*. 115, 1–18.

De Rosa R., Dominici R. & Sonnino M. 2001: Syn-sedimentary volcanism evidences in the Pleistocenic succession of the Mesima Graben (central-northern Calabria). *Il Quaternario* 14, 2, 81–91. (in Italian with English abstract),

De Rosa R., Dominici R. & Sonnino M. 2002: Stratigraphy and origin of volcaniclastic Plio-Pleistocene deposits from southwestern Calabria. Plinius, Suppl. it. *Eur. J Mineral.* 28, 141–142. (in Italian with English abstract).

De Rosa R., Guillou H., Mazzuoli R. & Ventura G. 2003: New unspiked K-Ar ages of volcanic rocks of the central and western sector of the Aeolian Islands: reconstruction of volcanic stages. *J. Volcanol. Geotherm. Res.* 120, 161–178.

De Rosa R., Dominici R., Donato P. & Barca D. 2008: Widespread syn-eruptive volcaniclastic deposits in the Pleistocene basins of South-Western Calabria. *J. Volcanol. Geotherm. Res.* 177, 155–169.

Di Stefano A. & Lentini F. 1995: Stratigraphic reconstruction and paleotectonic significance of Plio-Pleistocene deposits from the Tyrrhenian margin between Villafranca Tirrena and Faro villages (NE Sicily). *Studi Geologici Camerti* 2, 219–237. (in Italian with English abstract)

Dolfi D., De Rita D., Cimarelli C., Mollo S., Soligo M. & Fabbri M. 2007: Dome growth rates, eruption frequency and assessment of volcanic hazard: Insights from new U/Th dating of the Panarea and Basiluzzo dome lavas and pyroclastics, Aeolian Islands, Italy. *Quaternary Internat.* 162, 182–194.

Ferranti L., Antonioli F., Mauz B., Amorosi A., Dai Pra G., Mastronuzzi G. & Verrubbi V. 2006: Markers of the last interglacial sea-level high stand along the coast of Italy: tectonic implications. *Quaternary Internat.* 145, 30–54.

Fisher R.V. 1961: Proposed classification of volcaniclastic sediments and rocks. *Geol. Soc. Am. Bull.* 72, 1409–1414.

Fisher R.V. 1966: Rocks composed of volcanic fragments. *Earth Sci. Rev.* 1, 287–298.

Fisher R.V. & Schmincke H.U. 1984: Pyroclastic Rocks. *Springer-Verlag*, New York, 1–472.

Gaetani M. & Sacca' D. 1984: Bathyal brachiopods of Sicily and Calabria in the Pliocene and Pleistocene. *Rivista Italiana di Paleontologia e Stratigrafia* 90, 3, 407–458. (in Italian).

Gargano C. 1994: Geological map of Messina and NE sector of the Peloritani Mountains (NE Sicily), scale 1:25.000. *S.El.Ca*., Florence. (in Italian).

Heinicke J., Italiano F., Maugeri R., Merkel B., Pohl T. & Schipeck M. 2009: Evidence of tectonic control on active arc volcanism: The Panarea-Stromboli tectonic link inferred by submarine hydrothermal vents monitoring (Aeolian arc, Italy). *Geophys. Res. Lett*. 1–36.

Heiken G.H. &Wohletz K.H. 1985: Volcanic Ash. *University of California Press*, Berkeley, 1–246.

Heiken G.H. &Wohletz K.H. 1991: Fragmentation processes in explosive volcanic eruptions. In: Fisher R.V. & Smith G. (Eds.): Sedimentation in Volcanic Settings. *Society of Sedimentary Geology*, 45, 19–26.

Houghton B.F. & Wilson C.J.N. 1989: A vesicularity index for pyroclastic deposits. *Bull. Volcanol.* 51, 451–462.

Hornung J. & Aigner T. 2002: Reservoir architecture in a terminal alluvial plain: an outcrop analogue study (upper Triassic, southern Germany) part ii: cyclicity, controls and models. *J. Petrol. Geol.* 25, 2, 151–178.

Inmann D.L. 1952: Measures for describing the size distribution of sediments. *J. Sed. Res.* 22, 3, 125–145.

Italiano F., De Santis A., Favali P., Rainone M.L., Rusi S. & Signanini P. 2014: The Marsili Volcanic Seamount (Southern Tyrrhenian Sea):a potential offshore geothermal resource. *Energies* 7, 4068–4086.

Kamenov G.D., Dekov V.M., Willingham A.L, Savelli C. & Belluci L.G. 2009: Anthropogenic Pb in recent hydrothermal sediments from the Tyrrhenian Sea: implications for seawater Pb control on low-temperature hydrothermal systems. *Geology* 37, 111–114.

Keller J., Ryan W.B.F., Ninkovich D. & Altherr R. 1978: Explosive volcanic activity in the Mediterranean over the past 200.000 yr as recorded in deep sea sediments. *Geol. Soc. Amer. Bull.* 89, 591–604.

Kézirian F. 1992a: Evolution tectono-sedimentarie post nappes des MontsPeloritains (Sicile, NE). *Mém. De Geol. IGAL* 49, 1–260.

Kézirian F. 1992b: Evolution tectono-sedimentarie des series Oligocènes et Pléistocènes des Monts Peloritains (Sicile septentrionale). *Mém. Géol. IGAL* 49, 1–259.

Knott S. D. & Turco E. 1991: Late Cenozoic kinematics of the Calabrian arc, southern Italy. *Tectonics* 10, 6, 1164–1172.

Kokelaar P. 1986: Magma-water interactions in subaqueous and emergent basaltic volcanism. *Bull. Volcanol.* 48, 275–289.

Le Bas M.J., Le Maitre R.W., Streckeisen A. & Zanettin B. 1986: A chemical classification of volcanic rocks based on the total-alkali-silica diagram. *J. Petrol.* 27, 745–750.

Lentini F., Carbone S., Catalano S., Di Stefano A. Gargano C., Romeo M., Strazzulla S. & Vinci G. 1995: Sedimentary evolution in basins in mobile belts: Examples from Tertiary terrigenous sequences of the Peloritani Mts. *Terra Nova* 161–170.

Lentini F., Carbone S., Catalano S. & Grasso M. 1996: Elements for structural reconstruction of Eastern Sicily. *Mem. Soc. Geol. It.* 51, 179–195. (in Italian with English abstract).

Lentini F., Di Stefano A. & Strazzulla S. 1997: The Middle-Late Miocene terrigenous deposits of the Peloritani Mounts. In: *Interim Colloquium R.C.M.N.S.*: Neogene Basins of the Mediterranean Region — Controls and Correlation in Space and Time. Catania, 14–18.

Lentini F., Catalano S. & Carbone S. 2000: Geological Map of the Messina Province, scale 1:50.000. Provincia Regionale di Messina, Assessorato Servizio Territorio. *Servizio Geologico d'Italia*. (in Italian).

Leyrit H., Pompilio M., Berrier P., Lanzafame G. & Toussaint T. 1998: Sur l'origine eolienne des volcanoclastites pleistocenes du nord-est de la Sicile. RST98 — *Reunion des Sciences de la Terre Congrès*, Brest 31 mars–3 avril, 149.

Lombardo G. 1980: Stratigraphy of the Pleistocene deposits from NE Sicily. *Acc. Gioenia Sc. Nat. Catania* 12, 84–113 (in Italian).

Loreto M.F., Italiano F., Deponte D., Facchin L. & Zgur F. 2015: Mantle degassing at the top of an unknown submarine volcano in the SE Tyrrhenian Sea. *Terra Nova* 27, 195–205.

Lucchi F., Keller J. & Tranne C. A. 2013: Regional stratigraphic correlations across the Aeolian archipelago (southern Italy). In: Lucchi F., Keller J. & Tranne C.A. (Eds.): The Aeolian Islands Volcanoes. *Geological Society* 37, 55–81.

Lupton J., de Ronde C., Sprovieri M., Baker E. T., Bruno P. P., Italiano F. & Greene R. 2011: Active hydrothermal discharge on the submarine Aeolian Arc. *J. Geophys. Res.: Solid Earth* 116, 1978–2012.

Malinverno A. & Ryan W. B. 1986: Extension in the Tyrrhenian Sea and shortening in the Apennines as result of arc migration driven by sinking of the lithosphere. *Tectonics* 5, 2, 227–245.

Marani M.P. & Gamberi F. 2004: Distribution and nature of submarine volcanic landforms in the Tyrrhenian Sea: the arc vs the backarc. *Mem. Descr. Carta Geol. d'It.* 64, 109–126.

McDonough W.F., Sun S., Ringwood A.E., Jagoutz E. & Hofmann A.W. 1992: K, Rb and Cs in the earth and moon and the evolution of the earth's mantle. *Geochim. Cosmochim. Acta* 56, 1001–1012.

McPhie J., Doyle M. & Allen R. 1993: Volcanic textures. A guide to the interpretation of the tectures in volcanic rocks. *Centre for Ore Deposit and Exploration Studies, CODES Key Centre, University of Tasmania*, Hobart, 1–196.

Monaco C. & Tortorici L. 2000: Active faulting in the Calabrian arc and eastern Sicily. *J. Geodyn.* 29, 3, 407–424.

Mulder T. & Alexander J. 2001: The physical character of subaqueous sedimentary density flows and their deposits. *Sedimentology* 48, 269–299.

Narcisi B. & Vezzoli L. 1999: Quaternary stratigraphy of distal tephra layers in the Mediterranean - an overview. *Glob. Planet. Change* 21, 31–50.

Paterne M., Guichard F. & Labeyrie J. 1988: Explosive activity of the South Italian volcanoes during the past 80,000 years as determined by marine tephrochronology. *J. Volcanol. Geotherm. Res.* 34, 153–172.

Pearce J.A. &Cann J.R. 1973: Tectonic setting of basic volcanic rocks determined using trace element analyses. *Earth Planet. Sci. Lett.* 19, 290–300.

Peccerillo A. & Taylor S.R. 1976: Geochemistry of Eocene calc-alkaline volcanic rocks from the kastamonu Area, Northern Turkey. *Contrib. Mineral. Petrol*. 30, 227–256.

Peccerillo A. 2005: Plio-Quaternary Volcanism in Italy: Petrology, Geochemistry, Geodynamics. *Springer*, Heidelberg, 1–365.

Peccerillo A., De Astis G., Faraone D., Forni F. & Frezzotti M.L. 2013: Compositional variations of magmas in the Aeolian arc: implications for petrogenesis and geodynamics. In: Lucchi F., Keller J. & Tranne C.A. (Eds.): The Aeolian Islands Volcanoes. *Geol. Soc., London, Memoirs* 37, 491–510.

Peccerillo A. & Frezzotti M.L. 2015: Magmatism, mantle evolution and geodynamics at the converging plate margins of Italy. *J. Geol. Soc. London* 172, 407–427.

Pino P., Baldanza A., Belfiore C., Di Bella M., Sabatino G., Triscari M. 2007a: Pleistocene clay formations in the Messina country (N.E. Sicily): a stratigraphic review. FIST 2007, Rimini, Epitome 2, 401.

Pino P., Belfiore C., Casella S., Di Bella M., Rasa' R., Sabatino G., Tripodo A. & Triscari M. 2007b: Interbedded ash levels in pleistocenic clay formations of the Thyrrenian coast of Sicily: possible archaeometric implications. *Geoitalia 2007, Epitome* 2, 343–344.

Pouclet A., Horvath E., Gabris G. & Juvigné E. 1999: The Bag tephra, a widespread tephrochronological marker in Middle Europe: chemical and mineralogical investigations. *Bull. Volcanol*. 60, 265–272.

Pyle D.M., Van Andel T.H., Paschos P. & Van Den Bogaard P. 1998: An exceptionally thick middle Pleistocene tephra layer from Epirus, Greece. *Quat. Res*. 49, 280–286.

Rio D., Raffi I. & Villa G. 1990: Pliocene–Pleistocene calcareous nannofossil distribution patterns in the Western Mediterranean. In: Kastens K.A., Mascle J., et al. (Eds.): *Proceedings of the Ocean Drilling Program, Scientific Results*, 107, 513–532.

Romagnoli C. 2013: Characteristics and morphological evolution of the Aeolian volcanoes from the study of submarine portion. In: Lucchi F., Keller J. & Tranne C.A. (Eds.): The Aeolian Islands Volcanoes. *Geological Society*, 37, 13–26.

Romagnoli C., Casalbore D., Bortoluzzi G., Bosman A., Chiocci F.L., D'Oriano F., Gamberi F., Ligi M. & Marani M. 2013: Bathy-morphological setting of the Aeolian Island. In: Lucchi F., Keller J. & Tranne C.A. (Eds.): The Aeolian Islands Volcanoes. *Geological Society*, 37; 27–36.

Savelli C. 2002: Time–space distribution of magmatic activity in the western Mediterranean and peripheral orogens during the past 30 Ma (a stimulus to geodynamic considerations). *J. Geodynamics* 34, 99–126.

Savelli C. 1984: Evolution of cenozoic volcanism (from 29 My to present) in the Tyrrhenian Sea and in the surroundig areas: geochronological hypothesis on oceanic spreading phases. *Mem. Soc. Geolog. It.* 27, 111–119. (in Italian with English abstract).

Selli R., Lucchini F., Rossi P.L., Savelli C. & Del Monte M. 1977: Geological, petrochemical and radiometric data on central-Tyrrhenian volcanoes. *Giornale di Geologia* 412, 221–246. (in Italian).

Serpelloni E., Faccenna C., Spada G., Dong D. & Williams S. D. 2013: Vertical GPS ground motion rates in the Euro Mediterranean region: New evidence of velocity gradients at different spatial scales along the Nubia Eurasia plate boundary. *J. Geophys. Res.: Solid Earth* 118, 11, 6003–6024.

Schmidt R., Van Den Bogaard C., Merkt J. & Muller J. 2002: A new Late glacial chronostratigraphic tephra marker for the south-eastern Alps: The Neapolitan Yellow Tuff (NYT) in Langsee (Austria) in the context of a regional biostratigraphy and palaeoclimate. *Quater. Int.* 88, 45–46.

Sheridan M.F. & Wohletz K.H. 1983: Hydro-volcanism: basic considerations and review. *J. Volcanol. Geotherm. Res.* 17, 1–29.

Sprovieri R., Di Stefano E., Howell M., Sakamoto T., Di Stefano A. & Marino M. 1998: Integrated calcareous plankton biostratigraphy and cyclostratigraphy at Site 964. In: Robertson A.H.F., Emeis K.C., Richter C. & Camerlenghi A. (Eds.): *Proceedings of the Ocean Drilling Program*, *Sci. Results*, 160, 155–165.

Stix J. 1991: Subaqueous, intermediate to silicic composition explosive volcanism: a review. *Earth Sci. Rev.* 31, 21–53.

Sun S. & McDonough H.W.F. 1989: Chemical and isotopic systematics of oceanic basalts: implications for mantle composition and processes. In: Saunders A.D. & Norry M.J. (Eds.): Magmatism in ocean basins. *Geol. Soc. London Spec. Publ*. 42, 313–345.

Tansi C., Muto F., Critelli S. & Iovine G. 2007: Neogene-Quaternary strike-slip tectonics in the central Calabrian Arc (southern Italy). *J. Geodyn.* 43, 3, 393–414.

Toussaint T., Leyrit H. & Barrier P. 1999: Les depots volcanoclastiques Pléistocenes de Calabre et de Sicile: origine, dynamique et mode de depot. 7éme Congrès Français de Sédimentologie — Livre des résumés. *Publ. ASF*, Paris, 33, 301–302.

Trua T., Serri G., Marani M., Renzulli A. & Gamberi F. 2002: Volcanological and petrological evolution of Marsili Seamount (southern Tyrrhenian Sea). *J. Volcanol. Geotherm. Res.* 114, 3, 441–464.

Trua T., Manzi V., Roveri M., Artoni A. 2010: The Messinian volcaniclastic layers of the Northern Apennines: evidence for the initial phases of the Southern Tyrrhenian spreading? *Ital. J. Geosci.* 129, 2, 269–279.

Van Dijk J.P. & Scheepers, P.J.J. 1995: Neotectonic rotations in the Calabrian Arc; implications for a Pliocene-Recent geodynamic scenario for the Central Mediterranean. *Earth Sci. Rev.* 39, 3, 207–246.

Ventura G., Vilardo G., Milano G. & Pino N.A 1999: Relationships among crustal structure, volcanism and strike-slip tectonics in the Lipari-Vulcano volcanic complex (Aeolian Islands, Southern Tyrrhenian Sea, Italy). *Phys. Earth Planet. Int*. 116, 31–52.

Violanti D., Bonfiglio L. & Sacca' D. 1987: Pleistocene foraminifera and paleoenvironmental interpretations in an outcrop of NE Sicily (Rometta, Messina). *Riv. It. Paleont. Strat.* 93, 2, 251–286. (in Italian).

Violanti D. 1988: The Plio-Pleistocene foraminifera of Capo Milazzo. *Boll. Mus. Reg. Sci. Nat.* Torino, 6, 2, 359–392 (in Italian).

Violanti D. 1989: Plio-Pleistocene foraminifera from northern side of Peloritani Mountains: biostratigraphic and paleoenvironmental analysis. *Riv. It. Paleont. Strat.* 95, 2, 173–216. (in Italian).

Westaway R. 1993: Quaternary uplift of southern Italy. *J. Geophys. Res.* 98, 21741–21772.

Wohletz K.H. 1983: Mechanism of hydro-volcanic pyroclastic formation: grain-size, scanning electronic microscopy, and experimental data. *J. Volcanol. Geotherm. Res*. 17, 31–36.

Wohletz K.H. 1987: Chemical and textural surface features of pyroclasts from hydro-volcanic eruption sequences. In: Marshall J.R. (Ed.): Clastic Particles. *Van Nostrand Reinhold*, New York, N.Y., 79–98.